

Determination Of Thermal Properties Of Mineral Wool Insulation Materials For Use In Full-Scale Fire Modelling

by

Nicole Nagy

A thesis
presented to the University of Waterloo
in fulfillment of the
thesis requirement for the degree of
Master of Applied Science
in
Mechanical and Mechatronics Engineering

Waterloo, Ontario, Canada, 2020

© Nicole Nagy 2020

I hereby declare that I am the sole author of this thesis. This is a true copy of the thesis, including any required final revisions, as accepted by my examiners.

I understand that my thesis may be made electronically available to the public.

Abstract

Temperature-dependent materials properties are required for use in many contexts in fire safety engineering. While property values for many materials do exist, we often are limited in our understanding of how representative a given set of materials properties is for the application of interest. Thus, more work is needed to critically evaluate the measurement methods used, data obtained, and interpretation of the values in terms of their use in subsequent engineering applications. This research evaluates methods for determining thermal conductivity, density, mass loss, emissivity, porosity and specific heat capacity as functions of temperature of mineral wool insulation materials. These thermophysical properties will be applied to detailed heat and mass transfer modeling of the response of wall assemblies to realistic fire exposures. Use of the properties in more detailed models will, in turn, provide additional insight into the potential behavior of structural components during a fire for the purpose of occupant egress planning and firefighter safety.

The ability to model thermophysical degradation of materials is extremely important when assessing response of assemblies to the wide range of temperatures characteristic of a real fire exposure. Development of consistent methods for analysis and interpretation of the thermophysical properties of each element of the assembly will also guide testing of new, or previously untested, construction materials. Further, in order to develop a model of the response of the full assembly, it is necessary to determine appropriate parameters and properties required as input to submodels developed for the behavior of each material and those must accurately reflect the thermal and mass transfer processes taking place in that material. The objective of this study is to establish a set of methods for accurately characterizing the thermophysical response of construction materials as a function of temperature across a range of temperatures that would be encountered during exposure to real fire events.

Currently, one of the most common practices is to model heat transfer in a material using effective thermophysical properties for that material. This can involve estimating one or more properties at a set value of temperature (often room temperature or an average value between room and fire temperature) or combining two or more properties into

a single effective value as needed for input to the model. Such treatments are approximations intended to simplify the modeling process. It is well known that material properties change as a function of temperature, however, determination of properties such as density, specific heat, and thermal conductivity as functions of temperature is time consuming and is oftentimes inconsistent, depending on the material of interest and application. Some problems include the difficulty in preparation of specimens that are representative of the actual application of the material, as well as the variation of property data depending on the methods and/or heating regimes used in their determination. The wide range of materials commonly used in construction, each with distinct temperature response characteristics, also presents a challenge, making it difficult to develop universal methods for characterization that can be easily applied to every material.

In this research, physical and chemical properties of mineral wool insulation are first obtained using common practices listed in the literature, such as thermo-gravimetric analysis (TGA), and differential scanning calorimetry (DSC), as well as experiments designed by the writer. These reference values are then compared to values obtained using alternative or modified methods, as well as different test parameters, such as heating regimes or specimen preparation, designed to explicitly measure phenomena that are not specified through current property values. For example, from TGA experiments mass loss as a function of temperature is measured, which provides an estimate for density of a material as a function of temperature. Through the mass loss rate curve, temperatures at which thermally induced reactions are taking place can be identified, which advises on how to model that particular material in the temperature range of interest. From DSC test data, the specific heat capacity is calculated. The specific heat and density will then be used in combination with other results to estimate the thermal conductivity. Finally, properties measured using the various methods will be used as input into one-dimensional or more complex models of small-scale tests and full-scale wall fire experiments to predict the response of the assembly. New methods will be further interpreted in terms of their differences to current methods and those methods that provide the best representation of observations seen in the tests will be recommended as the methods to be used in future characterization of construction materials in this context.

Acknowledgements

Thank you to my family and friends for supporting me moving to Ontario to pursue my studies at the University of Waterloo, and to everyone who was there for me during my time as a graduate student. This degree would not have been possible without the funding support and expertise from ROCKWOOL® – thank you for being available to answer questions and to offer advice throughout the project. I would also like to thank the technical staff at the University of Waterloo in the Department of Mechanical and Mechatronics Engineering for assisting me with many aspects of my research.

I was given so many valuable opportunities by my supervisor, Professor Beth Weckman, to travel and learn about fire safety all over the world. I would like to thank Beth not only for teaching me and guiding my learning, but for her patience while I completed my thesis. My studies with Beth made it possible to be hired as a police officer before fully completing my thesis.

Table of Contents

Declaration	ii
Abstract	iii
Acknowledgements	v
List of Figures	ix
List of Tables	xi
1 Introduction	1
2 Background	7
2.1 Standard Fire Test Methods	7
2.2 Models and Correlations	14
2.3 Characterizing Construction Materials	16
2.3.1 Temperature Measurement Methods	17
2.3.2 Measurements of Mass Change	18
2.3.3 Volume Change and Porosity	21

2.3.4	Specific Heat Capacity	23
2.3.5	Emissivity	26
2.3.6	Thermal conductivity	28
3	Methodology	31
3.1	Materials	32
3.2	Temperature Measurement	32
3.3	Furnace Testing	33
3.3.1	Calculations	35
3.3.2	Porosity	36
3.4	Characterization Experiments	37
3.4.1	Thermogravimetric Analysis	38
3.4.2	Specific Heat Capacity	39
3.4.3	Emissivity	40
3.4.4	Thermal Conductivity	41
3.5	Two-Dimensional Axi-Symmetric Model	43
4	Results and Discussion	46
4.1	Furnace Testing	46
4.1.1	ASTM E136 Test Results	46
4.1.2	Interior Degradation and Shrinkage	50
4.2	Characterization Experiments	54
4.2.1	Thermogravimetric Analysis	54
4.2.2	Specific Heat Capacity	57

4.2.3	Porosity	59
4.2.4	Emissivity	59
4.2.5	Heat Conduction Experiment	61
4.3	Two-Dimensional Axi-Symmetric Model	68
5	Conclusions	76
5.1	Furnace Testing	76
5.2	Characterization Tests	77
5.3	Two-Dimensional Axi-Symmetric Model	78
	References	79

List of Figures

2.1	TGA Testing Equipment.	19
2.2	DSC Specimens and Crucibles.	24
2.3	Emissivity Testing Equipment.	28
3.1	Images of test specimens before being placed in furnace.	33
3.2	Tube Furnace.	35
3.3	TGA Testing Equipment.	39
3.4	Cone Calorimeter Thermalconductivity Test Setup.	41
3.5	Thermocouple Placement	42
3.6	Specimen	42
4.1	Percent mass loss of specimens tested at various furnace temperatures.	47
4.2	Average temperatures of centre and surface throughout a test.	48
4.3	Temperature difference between surface and centre temperatures of specimens at various furnace temperatures.	49
4.4	Interior Degradation of Tube Furnace Specimens.	51
4.5	Cubic furnace specimens – 500°C for various exposure times.	52
4.6	Cubic furnace specimens – 750°C for various exposure times.	52

4.7	TGA Test Results	55
4.8	DSC - Specific Heat Results	58
4.9	Emittance as a function of wavelength.	60
4.10	Cone test plots legend.	61
4.11	ROCKWOOL Safe [®] under 50kW/m ² exposure	62
4.12	ROCKWOOL Safe [®] under 35kW/m ² exposure	63
4.13	ROCKWOOL Safe [®] under 25kW/m ² exposure	64
4.14	Percent Mass Loss During Cone Tests - ROCKWOOL Safe [®]	68
4.15	Comparison between modelled and experimental results – 25Kw/m ²	74
4.16	Comparison between modelled and experimental results – 50Kw/m ²	75

List of Tables

2.1	ASTM E119 Temperature–Time curve data.	12
3.1	Thermocouple Numbering	43
4.1	TGA Mass Loss Summary	56
4.2	Material Event Onset Temperatures	57
4.3	DSC Major Event Temperatures	58
4.4	Total Near-Normal Emittance	60
4.5	Temperatures Measured After 1 Hour During Heat Conduction Experiments (°C)	65
4.6	Material properties for the model	69
4.7	Percent Difference Analysis	71

Chapter 1

Introduction

Fire safety is one of the most critical aspects of a building design, and consequently certain fire resistance ratings are required for wall, ceiling, and floor assemblies within a structure or for a building as a whole. Next generation construction assemblies therefore need to show superior fire performance, particularly with respect to their overall fire resistance ratings, in concert with any improved thermal insulation capabilities necessary to address emerging energy stipulations. The National Building Code of Canada (NBCC) stipulates the overall fire performance requirements that must be met and test protocols that must be followed for structural assemblies to qualify for use in particular buildings based on their intended application [1]. In order to meet current building regulations, typical wall construction in Canada consists of a combination of wood framing and fiber or polymer insulation on the interior, with an oriented strand board backing and front face of gypsum board cladding for fire protection.

The fire resistance of a construction assembly is largely dictated by the performance of its constituent materials and the manner in which it is constructed. Before going to market, therefore, various components in a construction assembly are individually required to pass certain standard tests as outlined by the NBCC [1]. These certification tests can be expensive and time consuming and test facilities are limited. Added to this, certification tests are generally not well instrumented so that if a material or assembly fails to pass a

certain test, a manufacturer gains very little insight into the reasons for failure or, perhaps more importantly, obtains no data to guide modification of the design to ensure success of a future design.

At small-scale, some of the standard tests can be difficult to pass without advanced understanding of the behaviour of a particular material when exposed to heat. For example, one distinction made in the NBCC is that of a combustible versus non-combustible material [1]. In this instance, combustibility is determined by a standardized test method such as ASTM E136 [2] or CAN/ULC-2114 [3]. In essence, these are thermal-response tests wherein small specimens of a material are placed in a furnace at 750°C, and the temperature of the outside of the material is compared to the temperature of the centre of the material over time. If the centre temperature exceeds the surface temperature by a certain margin, the material is considered to be generating heat, and is classified as a combustible material even though it may not burn or even contribute to the overall heat release rate in a real fire situation.

At larger scale, the NBCC prescribes minimum fire resistance rating values for full-scale wall, ceiling, and floor assemblies [1]. These ratings are in units of time, and represent the time taken for a full-scale assembly to fail according to the stipulations set out in [4] and [5]. Typical values of fire resistance rating for residential construction scenarios [1] range from 30-120 minutes based on exposure of the assembly to a spatially uniform surface temperature distribution defined via a standardized fire temperature curve. Failure criteria are dependent on the assembly application, but for a wall for example, failure coincides with passage of flame or smoke to the unexposed side of the wall resulting in a temperature increase on the unexposed side to a certain extent [4,5]. A detailed description is located in Section 2.1. Although this test is widely used in North America and is a requirement in Canada [1], limitations in its applicability to real fire situations have been identified. There is a question of the accuracy of predicting real fire performance based on information from tests of isolated building materials or assemblies outside of their intended environment under thermal exposures not representative of those encountered in real fires. As well, there are issues related to the fire resistance ratings for buildings containing combustible materials that have a non-negligible effect on the fire exposure profile when compared

to the prescribed ASTM E119 time-temperature curve that is accepted in Canada [6]. As noted above as well, scientific interpretation of the results of large scale certification tests is hampered due to limitations in instrumentation and due to the fact that it is not realistic to perform a large number of these tests due to the dearth of test facilities, as well as the extremely high testing costs (approximately \$25,000/wall test and approximately \$5000/tunnel test).

Under the above regulatory framework, the need for individual materials to pass tests that do not directly relate to fire situations inhibits design and thus use of new materials that may perform very well in real fires. Instead, materials are engineered to simply pass certain tests and the impetus to understand how they would respond to realistic fire situations is removed. This, coupled with inherent gaps in our knowledge of the actual high temperature properties and behaviour of many building materials, also makes it difficult to predict specific impacts of each individual component on the overall fire performance of even a typical composite wall, ceiling or floor assembly in a real situation. Such factors greatly restrict development of new and innovative materials and assembly designs optimized for fire safety.

From a different perspective, the rate at which new construction materials are being developed has increased in recent years to a point that keeping up with the required fire performance testing standards becomes a challenge for the manufacturers. Many manufacturers are developing multiple new products at any given time, and therefore need to run and pass expensive and time-consuming certification tests before taking any of their products to market. If a new product does not meet the fire safety requirements on the first pass, the result is a costly cyclic redesign and re-testing procedure. Improved materials screening methods coupled with accurate computer modelling of the thermal response of construction materials will aid in the design process, allowing for development of smaller-scale, less expensive testing protocols in order to guide at least the early stages of the materials design process. This will lead to only the most promising materials advancing to the stage of standard certification testing and will lower overall testing costs since fewer repeat tests will be necessary. Ultimately, development of integrated experimental - computational materials and assembly design methodologies will lead to competitively priced

new products based on overall higher success rates for certification of these products for fire safety applications.

One key element in development of a new method for design and evaluation of construction assemblies for fire performance is to understand and model the behaviour of individual construction materials in realistic fire conditions. For this, the knowledge of the temperature dependent properties of each material is essential. To this end, properties of standard building materials such as gypsum and wood have been widely studied with the aim of developing universal models for their behaviour across a certain range of temperatures or under a specified incident heat flux [7, 8, 9, 10, 11]. Far fewer studies have focused on determining thermal properties of mineral wool and other insulating materials [12, 13], or insulation in wall assemblies [12, 13, 14, 15] under fire exposure, even though insulation is one of the main components of most construction assemblies. In general, current models of temperature dependent materials properties for any of the above materials are limited by over-simplified representations of the dynamic physical and chemical processes taking place in individual materials under heating and are even weaker in terms of representing how these phenomena lead to the observed behavior and response of a material in a fire.

Better understanding of the behaviour of building materials in general, and in particular insulating materials, during fire exposure is critical to development and evaluation of new products and applications as well as to development of next generation performance-based solutions for design of construction assemblies. As a first step in characterizing temperature dependent properties and response of materials, it can be advantageous to use small-scale fire performance test methods [9, 13, 16, 17] suitably adapted for research purposes. It remains a challenge, however, to represent the full scale thermal/fire response of a material or assembly using small-scale results, as there is a lack of established methodology with which to scale the results. This issue, taken together with the knowledge gaps listed above, limit the use of small scale fire test data when it comes to understanding the actual performance of materials in full-scale fires. Nonetheless, it has been shown that small scale testing can be extremely valuable during new product design and development cycles [18, 19]. Complementary to experimental testing, the ability to model the thermophysical response and potential degradation of the assembled materials under the wide range of temperatures

characteristic of fire exposure is also a key element in evaluation of new products for fire safety. This is a complex task, however, as there are many challenges with understanding, and thus also modelling, heat and mass transfer through even commonly used construction materials. Issues include difficulties in characterizing the detailed internal structure of the materials, and uncertainty in specifying global material properties such as thermal conductivity, density, and specific heat at elevated temperatures and also as the materials undergo thermo-chemical decomposition during exposure to heat. This motivates research efforts towards developing a consistent and complementary set of analytical test methods and computer modelling software with which to estimate the fire performance of various materials during the design phase of new material development for construction assemblies.

The overarching objective of the work outlined in this thesis is to contribute to the development of a new engineering tool which will assist engineers and the industrial research and development (R&D) community with recommending appropriate “next steps” in developing new building materials. The final tool will provide a faster and more cost effective method for testing or screening materials during the design process, which will consequently allow manufacturers to bring new products to market in less time. The tool will consist of two parts that directly guide the phases of this research. The first centres on determining a set of streamlined tests that can be used in characterization of key properties of materials across a range of temperatures. In the second stage, these will be coupled with development of models that can be used for estimation of the thermal response of the materials under certain exposures to heat. Specifically, this research focuses on determining which characterization methods are appropriate and efficient for estimation of key material properties while maximizing accuracy of the final data in terms of providing those properties that are needed as input for the final fire-materials response models.

To that end, the present research is based on the following specific objectives:

- To undertake a survey of existing and alternative methods for characterization of materials across the range of conditions encountered in real fires and using that information to identify candidate methods to be used in the assessment tool.
- Using the methods determined above, to conduct an experimental investigation of the

thermo-physical and chemical properties of two common types of building insulation over a temperature range similar to that experienced during a fire. The specific materials of interest in this thesis are ROCKWOOL ComfortBatt[®] and ROCKWOOL Safe[®] insulation products, which are mineral wool based materials used in commercial, industrial, residential, and marine insulation applications.

- To use the measured properties as input into a 2-D axisymmetric model for heat transfer in a larger test system. Comparison between predictions and experimental results are intended to provide further insight into the use of small-scale data in improved models for estimation of the thermal response of materials under exposure to heating characteristic of a range of different fire scenarios.

The data obtained will provide new insight into the general behaviour of two common construction insulation materials under heating, as well as important information to support development and testing of a two-dimensional axisymmetric model of heat transfer through slabs of each material. Over the longer term, the data will also aid in the creation of more detailed and advanced multi-physics models for prediction of heat and mass transfer through these, and similar, insulating materials in real fire situations.

In the following Chapter of this thesis, background information is presented and discussed. Following this in Chapter 3, the methods used in the experimental portion of the research are outlined and the model is described. Chapter 4 and 5 include results and conclusions found through the present study, as well as recommendations for future work.

Chapter 2

Background

The long term goal of this research is to contribute to the creation of an advanced multi-physics model for prediction of heat and mass transfer through insulating materials in real fire situations. For this, multiple methods for materials characterization were reviewed to determine a streamlined practice for materials characterization. A balance between cost effectiveness and efficiency was considered, along with common practices identified in the literature. This Chapter outlines the background and methods used for research in this thesis. Detailed descriptions of the methods and equipment used as well as explanations for why they were chosen are included.

2.1 Standard Fire Test Methods

Standardized testing and performance certification for construction materials is based on a series of test protocols that have been developed to ensure that materials meet certain minimum performance standards important for their intended application. Each material is therefore certified via a cross-section of standardized materials property and fire performance tests before they are released into the market. From the standpoint of R&D into new and innovative materials, however, repetitive testing of new formulations via certification tests during the early materials design and development phase poses multiple

challenges. These tests are time consuming and expensive and many of the test methods are only sparsely instrumented from the point of view of collecting detailed physical data through which to truly understand a materials response to thermal exposure. The cost becomes significant if a new formulation is initially unsuccessful in meeting the standard and a sequence of retesting is required to refine the formulation. Alternately, it can become a factor if a company is developing multiple products or families of products, all of which requiring individual testing to better understand the full spectrum of their fire performance.

Based on the above issues, this section explores different methods for characterizing construction materials in cost-effective ways at the materials development stage. The intent is that the methods chosen would be used to assist with developing materials that are successful in subsequently meeting the necessary standard fire certification tests for a particular application. To this end, important aspects of several key standard fire performance tests are described first. The discussion then presents a range of available small-scale characterization methods and assesses the viability of using these smaller scale techniques for determining materials characteristics that could be used to predict performance in the various certification tests and/or to investigate key aspects of large-scale fire behaviour.

Standard test methods form the basis of regulated means for measuring, testing, or comparing some aspect of the performance of a material or combination of materials. Ideally the standard methods are adaptable for use in a wide range of applications and to a variety of materials, and are reasonably accessible (or executable) by any manufacturer or laboratory. In reality, each country has certain, and different, overarching requirements in their local building codes and standards of practice related to fire performance of construction materials in order to ensure that a structure is fire-safe. These most often refer to requirements specified in terms of the results from one or more standard fire performance test methods. As discussed in the following sections, important examples of this relate to the designation of whether a particular building construction will be classified as combustible or non-combustible, as well as to the determination of a specified fire resistance rating of a building material or assembly.

ASTM E136

In terms of classification of materials with respect to their use in construction applications, the ASTM Standard Test Method for Behaviour of Materials in a Vertical Tube Furnace at 750°C (ASTM E136) is used to determine whether a material is combustible or non-combustible as specified in North American building codes [2]. Per ASTM E136, $38 \times 38 \times 51 \pm 2.5$ mm specimens are dried at $60 \pm 3^\circ\text{C}$ for between 24 – 48 hours, then placed in a dessicator to cool for a minimum of one hour prior to testing. One thermocouple is placed at the centre of the specimen, and another on the surface to monitor temperature of the specimen material throughout the test. The test furnace is stabilized to an interior temperature of $750 \pm 5.5^\circ\text{C}$ prior to inserting the specimen. Visual observation is used to assess the occurrence of flaming and/or smoking as a result of the specimen being heated.

The test commences once the specimen is placed inside the furnace, and continues until one of the following criteria for classification of combustibility is met:

- 30 minutes has elapsed;
- the specimen has visible flaming or smoking (classified as combustible); or
- the specimen temperature exceeds the furnace temperature by greater than 30°C (classified as combustible).

If the specimen survives the 30 minute duration (as specified by the criteria above) and does not lose more than 50% of its mass by the end of the test, the specimen material is deemed non-combustible as per the ASTM E136 standard. Alternately, the specimen will be classified as combustible if a mass loss of greater than 50% is recorded from beginning to end of the test or either of the conditions given in criteria 2 or 3 above is observed.

This test method explicitly states the following limitations in terms of its use for classifying combustibility [2]. It is stated that the test:

1. does not apply to laminated or coated materials,

2. is not suitable for use on materials that soften flow, melt, intumesce, or otherwise separate from the instrumentation required for this test,
3. does not provide a measure of an intrinsic property
4. does not provide a quantitative measure of heat generation or combustibility - simply serves as a test method with selected measures of combustibility
5. does not measure self-heating tendencies of materials
6. does not apply if specimen preparation requires the material of interest to be tested outside of the intended configuration for its use in the building application.
7. is limited by the fact that specimens have to be cut, assembled, or contained in a secondary container to facilitate testing.

Further, it is emphasized that results from this test method apply to the specific test apparatus and test conditions and are likely to vary when changes are made to one or more of the following: size, shape, or arrangement of specimen, distribution of organic content, exposure temperature, air supply, location or thermocouples.

This standard is convenient in that it is relatively inexpensive and can be done quickly. However, despite statement 6 above, the method does not assess a material in its intended configuration or environment and the specimen is restricted to a certain size, so that subject materials need to be cut, assembled, or placed in a secondary container. Therefore, there are a wide range of materials that cannot be tested by this standard. Even for materials that can be tested, the test provides no insight into the details of thermal response or breakdown of a material under exposure to heat. Further, potential inconsistencies arise because the material is tested outside of its intended environment. For example, in ASTM E136 insulation is tested on its own; however, it is not typically a stand-alone building material but instead is usually within walls, surrounded by other materials such as gypsum board and wood.

Arguments have been made that the ASTM E136 test is an outdated standard [20]. Babrauskas describes that, historically, categorizing construction components as “combustible” and “non-combustible” may have been reasonable when construction components were limited to items such as brick, steel, and wood. At present, however, there is such a vast selection of building components, that there needs to be a quantitative method for testing materials, rather than the categorical ASTM E136 test that determines “combustibility” based on a series of rather arbitrary threshold conditions. He suggests that flame spread methods such as flame spread limitation studies are ideal candidates for replacing the ASTM E136 test for combustibility, but also mentions that heat release rate methods are used more frequently. Either of these methods could potentially provide more detailed and even limited quantitative information regarding the product being tested, resulting in a deeper understanding of the material’s behaviour during heating and thus, in a realistic fire situation. The alternative tests also show promise in relating full scale to bench scale results [21]. As suggested by the objectives of the present research, an even higher level of detail might be derived from a combination of small-scale characterization methods for determining a specific set of material characteristics that could then be used to predict overall fire performance or to investigate key aspects of large-scale fire behaviour of the material or an assembly.

At the other end of the spectrum, one approach to testing materials in their intended configuration is through larger scale and more complex procedures such as ASTM E119 – Standard Test Methods for Fire Tests of Building Construction and Materials, which is outlined in the following section.

ASTM E119

ASTM E119 is a fire test response standard that is commonly used for determination of fire resistance of full scale construction materials and assemblies. Individual materials or assembled walls, columns, floors and other building structures are tested at full scale by exposing them to a standard time temperature fire exposure curve [5] as shown in Table 2.1, for specified periods of time.

Temperature (°C)	Time
538	5 min
704	10 min
843	30 min
927	1 hr
1010	2 hr
1093	4 hr
1260	≥8 hr

Table 2.1: ASTM E119 Temperature–Time curve data.

For the ASTM E119 test, wall specimens with minimum exposed area of 9m² and with neither height nor width less than 2.7m, are mounted in one wall of a large furnace. The gas burners in the furnace are programmed to follow the exposure curve specified in Table 2.1 and to maintain the interior temperatures to within 10% of the specified values throughout the test. Control temperatures are taken as an average of nine thermocouples placed 152 mm away from the exposed side of the test specimen and symmetrically distributed throughout the furnace. Readings are taken every five minutes during the first two hours of a test, and if the test exceeds two hours, readings are continued every ten minutes after the initial two hours. The unexposed surface of a test specimen is instrumented with no fewer than nine thermocouples which are sampled with a time resolution of 30 seconds.

A cotton pad test is used to determine whether the wall specimen has allowed the passage of gases hot enough to ignite a standardized cotton pad. This establishes if a specimen cracks or otherwise allows passage of hot gases during the test. Once the furnace portion of the ASTM E119 fire resistance test is complete, a hose stream test is commenced to determine the residual integrity of the test specimen. This test is outlined in the ASTM E2226 Standard Practice for Application of Hose Stream, which prescribes water pressure, duration, and pattern of application of water to the wall assembly [22].

Since the ASTM E119 test is primarily used to determine a fire resistance rating for the tested assembly under controlled conditions, it is completed if:

- The test specimen withstands the test without passage of flame or gases hot enough

to ignite a cotton pad for a period of time equal to that for which classification is desired.

- The test specimen withstands the fire and hose stream test as specified, without passage of flame, or gases hot enough to ignite the cotton pad, or of passage of water from the hose stream.
- The test specimen does not develop any openings that permit a projection of water from the hose stream beyond the unexposed surface during the time of the hose stream test.
- Transmission of heat through the wall during the test results in a temperature increase of less than 139°C on the unexposed side relative to its initial temperature

The ASTM E119 test is a time consuming and costly test to complete. The temperature time curve outlined in Table 2.1 is widely accepted to be a reasonable exposure for determining the fire resistance of wall and floor assemblies; however, it provides a uniform temperature exposure to the assembly so it is not representative of the spatially varying thermal exposure representative of a real fire [6]. Due to the exposure, as well as the very limited instrumentation that is specified in the standard methodology, the ASTM E119 test does not, nor is it intended to, provide detailed knowledge or understanding of the thermal or fire response of the various materials or assemblies being tested.

From the overview of ASTM E136 and ASTM E119 above, while materials and assemblies must pass such tests in order to meet category classifications and code requirements for certain applications, alternative methods must be applied to provide researchers and industry with more realistic insight into the detailed fire performance of materials and products during research, optimization or new product development.

On the other hand, due to the importance of the ASTM E119 test for certification of fire resistance ratings of assemblies in buildings, numerical and experimental studies into the response of common construction materials, such as concrete, wood, and steel, and various assemblies to the standard ASTM E119 temperature time curve have been conducted. In

contrast, fewer investigations have involved experimental and numerical analysis of real structures under real fire exposures [6]. A review of pertinent models and correlations is included in the following section.

2.2 Models and Correlations

Modelling fire scenarios requires the application of complex physics and consideration of key aspects of fire behaviour, translation of those to define thermal exposures to materials and assemblies, and knowledge of a range of materials properties to facilitate modelling of the material response to that exposure. Properties such as thermal conductivity (k), specific heat (c_p), and density (ρ) are core properties needed to describe material's response to thermal exposure via fundamental models of heat transfer. When modelling the high temperature scenarios encountered in fires, however, high temperature material properties or reasonable correlations are required in order to obtain realistic results. The process of determining these requires in depth understanding of the fire environment as well as the materials involved in the fire in order to accurately simulate the situation being studied. In most cases, this knowledge cannot be obtained from standard tests such as those mentioned above but instead must be determined via additional testing of individual materials in test configurations specifically tailored for the purpose. The reality at present, unfortunately, is that the literature yields limited results for the necessary high temperature properties of materials, and those that are available for construction materials show significant variability [23,24,25].

Attempts have been made, with the motivation of reducing the need for full scale fire testing, to create appropriate combinations of small scale tests [26] and computer models of fire scenarios [15,26,27,28,29,30]. The models consider heat and sometimes mass transfer through a multicomponent assembly in one, two, or three dimensions, most often using finite difference or finite element methods [15,26,27,28,29,30]. No model is currently able to address the totality of a fire scenario as this would require representation of the time and spatially varying flow of hot gas and radiation from the fire. This would need to

be simulated in a realistic fire compartment properly interconnected with models for the temperature dependent properties of all the materials as well as the heat transfer through the surrounding materials. Due to this complexity, simplifications such as representing the fire exposure as a constant average value of temperature or heat flux, or by using a standard time-temperature curve (such as that found in ASTM E119 [5]), are therefore used in many models that currently exist. In [31], an objective of the research was to obtain effective thermal conductivity values as it is a desired quantity for simplified practical fire resistance design – this speaks to the complexity of using temperature dependent material property values. Thermal conductivity for the purpose of modelling was approximated by [32] as a linear curve fit in combination with a third order representation past a certain temperature. Models with these sorts of simplification may be able to predict steady state temperature profiles reasonably well, however, they fall short in the areas of predicting the potential for damage of materials as a result of time and/or spatial variations in the exposure of wall cladding or other interior materials as one would observe in a real fire.

Both large scale testing and detailed design models for material response during a fire are limited by critical gaps in knowledge. These include consistent information on temperature dependent material properties as well as clear identification of damage thresholds and time and modes of failure for different materials. For example, phenomena such as the break down of gypsum cladding during a real fire is not well studied or understood [9, 12, 15, 16]. Additional difficulties arise in conjunction with the uncertainty associated with scaling test results and time dependent properties of materials from small to larger situations, as well as any variability of properties due to varying formulations of the “same” material across the range of different manufacturers.

To address some of these, temperature dependent properties of gypsum and wood have been studied fairly extensively [7, 8, 9, 10, 11, 23, 33], including studies focused on improved correlations for the material properties [8, 9, 10, 11, 16] as well as other more specific processes. In contrast, however, there are few studies that focus on the thermal response of insulating materials [12, 13] and insulation in wall assemblies [12, 13, 14, 15]. To build on this previous research, establishing methods for determination of consistent, accurate, and reliable materials property data is a main goal of the present research. Results from this

research will provide researchers and industry with initial data and new tools by which to gain far more insight into the fire performance of their products during development, which will greatly assist in bringing products through the certification process and to market. In order to do this, a series of small-scale, cost-effective tests that can accurately characterize the behaviour of construction materials in fire scenarios such as that mimicked in ASTM E119 are developed, and complementary modelling techniques are explored. The material properties that are determined will facilitate more accurate modelling of the properties of these materials in fire situations and the resultant methods will give new insight and understanding of the behavior of various materials across a wide range of temperatures.

2.3 Characterizing Construction Materials

There are many challenges with finding thermophysical properties of materials. One major restriction in determining these properties arises due to limitations in both test equipment and appropriate testing methodologies. For example, there are many methods available for finding thermophysical property values (k , c_p , ρ), under a given constant temperature conditions (most often ambient temperature) but far fewer appropriate for determination of temperature dependent properties across the wide range of temperatures encountered during a fire. When experimentally testing materials, consideration must be given to methods necessary for sample preparation as well, since it is usually desirable to accurately represent the configuration of the material in its intended application when finding characteristic material properties. In this regard, some methods require testing a powdered specimen rather than a solid piece of material, and many tests are done on very small samples of material. When interpreting the results, this brings into question how representative the property values obtained from such tests can actually be, when in a real fire scenario the material is in a different form and configuration and at much larger scale. The discussion below outlines methods referenced in the literature related to measurement of temperature, density, porosity, specific heat, emissivity and thermal conductivity of materials as these have consistently been identified as key parameters in fire research. In the Section following, the specific methods chosen for the present research are described in more detail

as well.

2.3.1 Temperature Measurement Methods

Various fire performance standard test methods require accurate temperature measurements of test materials to determine whether the standard has been met [2, 3, 5]. In addition, research in materials science uses temperature measurements to help understand the behaviour of materials of interest at various temperatures [6, 23]. Two common temperature measurement methods used for these purposes are thermocouples and infrared imaging. While there are many other temperature measurement methods (i.e., thermistors, IC semi-conductors, etc) the majority are not suitable for fire research due to the necessity of measuring up to the high temperatures encountered in realistic fire situations.

Thermocouples

Thermocouples are commonly used in fire research as a means for obtaining point temperature measurements [34]. A thermocouple wire consists of two dissimilar wires that are formed into a junction. When the temperature at the junction is changed, a voltage is generated via the Seebeck effect and this voltage can be correlated back to temperature. Different types of thermocouples use different conductors and have different lifespans, temperature ranges, and are used for a variety of applications.

Infrared Imaging

Infrared imaging has previously been used in fire characterization work [35, 36]. In this method, light emitted from an object in the infrared range of the electromagnetic spectrum is collected. The radiation emitted changes with temperature so that with appropriate calibration, infrared images can be analyzed to provide temperature measurements. As such, infrared imaging is useful in tracking temperature changes in two dimensions as a function of time by collecting multiple images taken from the same object in sequence

and analyzing them to determine a grid of instantaneous temperatures in each image [37]. The method is also advantageous because it remotely measures the temperature so avoids the need to mount a thermocouple or other temperature transducer to the surface of a material that is potentially changing under exposure to heat and also avoids exposure of the temperature transducers to high temperatures as well [37].

2.3.2 Measurements of Mass Change

Since materials undergo mass change while being exposed or involved in a fire, it is essential to characterize this detail when studying material behaviour under exposure to fire. Characterization of mass change can be done by methods such as thermogravimetric analysis (TGA) [23, 25, 38, 39, 40, 41]. TGA is a materials characterization method that uses a specified heating regime to heat a small, typically powdered specimen of a material of interest. A TGA apparatus is pictured in Figure 2.1. As the material is heated at a user specified rate, the mass of the specimen is recorded in order to obtain a relation between the change in specimen mass and temperature. The temperature range and the rate of heating/cooling that can be employed in TGA varies based on the capabilities of the specific instrument, and is user-adjustable based on the specific research objectives.

The temperature range as it applies to this research has to reflect temperatures similar to those seen in structure fires, potentially limited by abilities of available equipment. Ideally the heating rates and temperatures used would mimic those in a fire, though heating regimes in real fires have a high variability depending on the type of construction, fuel load inside the structure, ambient and ventilation conditions, etc. As a result, previous researchers have employed various strategies to investigate the thermal response of construction materials to heating. Key studies, with the methods employed and main results, are outlined below.

Researchers at NRC studied the mass loss of wood, gypsum and a limited number of insulation materials at temperatures between 20 – 1000°C using an electric oven as well as a DuPont 951 TGA [23, 25]. They conditioned their specimens at 40°C for 24 hours, and tested specimens that were powdered as well as cut sections of the materials. The



Figure 2.1: TGA Testing Equipment.

powdered/ground specimen masses ranged from 10 – 40mg, and were tested using TGA in a nitrogen atmosphere at heating rates of 5°C/min and 20°C/min. It was found that ROCKWOOL® insulation gradually decreased in mass across the entire range of heating, with approximately 94% mass remaining at the end of the heating period. In contrast, the mass loss rate for glass fibre insulation rapidly increased initially due to decomposition of the components, then remained approximately constant until the material melted.

Across the materials tested, it was observed that an increase in the rate of heating shifted the starting temperatures of a given process to higher values while also narrowing the temperature interval across which a given physical reaction proceeded. As a result, it is clear that the choice of heating interval and rate of heating are important parameters to consider in defining a protocol for use of TGA for measurement of mass change in construction materials.

Sjostrom and Jansson conducted combined TGA and DSC measurements on commercial stone wool board with a density of 170 kg/m³ using a STA F3 Jupiter from Netzsch [38]. They tested in an inert nitrogen environment at a heating rate of 5°C/min between room temperature and 1000°C. This group also ran the sample in air to account for the burn-

ing of the pyrolysis products from room temperature to 700°C, cooled the sample, then heated to 1050°C. Since their TGA was in conjunction with DSC measurements, their data illustrated two strong exothermal processes which they were able to model using simple tools.

Palumbo, Formosa, and Lacasta tested 5mg samples of bio-based thermal insulation materials in an inert nitrogen atmosphere using a TA Instruments SDT Q600 TGA [39] across the temperature range of 30°C – 600°C at a heating rate of 10°C/min. They observed distinct differences in mass loss rate between different binders that directly related to differences in thermal decomposition. Since only a single heating rate was employed, no insight into the effect of heating rate on decomposition could be determined. Further, while results were compared to organic foam insulations (polystyrene and polyurethane), no comparisons were drawn to any mineral wool insulation materials.

Chetehouna et al. used a TGA coupled with a mass spectrometer to study thermal degradation and kinetic parameters of new types of insulation materials composed of cereal straw with lime or plaster binder materials [40]. They used a Setsys 16/18 Setaram thermobalance coupled to a Balzers QMS 200 mass spectrometer to study 5mg specimens in an inert argon atmosphere in the range of ambient to 1000°C at a heating rate of 20°C/min. Results indicated that the thermal decomposition of the insulation, as measured by mass loss rate in a TGA, heavily depended on the nature of the binder used. Again only a single heating rate was employed and in this case no comparison was drawn to any other type of insulation material.

Park et al. developed a new approach to characterize the mass loss rate of gypsum board at high temperatures using 152mm x 50mm specimens [41]. They measured the mass of each specimen using a load cell as well as the dimensions of the specimens using CCD imaging and computer software before exposing each specimen to a constant temperature of between ambient and 900°C for 3 hours in an oven. The same mass/dimensional measurements were taken again after the heat exposure and curves were drawn of % mass loss and dimensional changes due to exposure across the range of temperatures. While no insulation materials were tested, the method did indicate small differences in mass loss with temperature across gypsum types. These were attributed to different additives in the

samples tested.

Mass loss characteristics of construction materials, including gypsum products, wood, and insulation materials, have been studied to determine thermal decomposition regimes for future use in fire modelling, however, there have been very few studies into the properties of insulation materials. In fact, there remain gaps as well as inconsistent results for many materials [23,41]. The proposed research includes looking at different material preparations and heating regimes to assess mass loss of the candidate insulation materials under different operating conditions. Heating rates and temperature ranges were chosen based on the aforementioned research as well as available equipment at the University of Waterloo.

2.3.3 Volume Change and Porosity

Volume change is important when studying the fire response of construction materials. Changes in volume and porosity as a result of exposure to heat can affect the resistance of materials to heat or lead to deformation, which, in turn, can lead to shrinkage which allows for the passage of hot gases to another compartment or can ultimately lead to the failure of a structure [41,42,43].

As noted above, while studying the mass loss rate of gypsum due to heating, Park also investigated the changes in volume of the gypsum samples during heating. For this they used dimensional analysis based on CCD camera images and observed significant differences in lateral contraction depending on the nature of the gypsum tested which was found to be strongly dependent on the composition of the additives [41].

Another method used for determining change in volume as a function of heat exposure is dilatometry. Dilatometers measure thermal linear expansion and contraction. The sample is placed in a furnace, and as the sample is heated, any expansion or contraction is detected by a strain gauge. The volumetric change as a function of temperature can be estimated by taking linear measurements along three different axes sequentially, assuming the material is not isotropically homogeneous. Alternately, assuming homogeneity in all directions, a single measurement of the linear shrinkage/expansion can be extended to three

dimensions to formulate a volume estimate as a function of temperature. This method is appropriate for solid materials and is used in the literature to determine volume change with temperature for materials such as gypsum [44] and concrete [45]. It does not appear to have been used for soft materials such as mineral wool insulation.

Researchers at NRC used a Theta Dilatory apparatus with a computer-controlled program to measure thermal expansion and contraction of gypsum materials [23, 25]. The temperature range explored was 20°C – 1000°C, and they used 30mm - 40mm long and 10x10 or 13x13 mm in cross-section specimens. The heating rate used was 10°C/min. Differences in measured values of thermal contraction in gypsum were attributed to time taken to dehydrate different samples coupled with changes in composition across gypsum boards tested. The contraction observed was further linked to changes in heat transfer through assemblies during heating, development of cracks and fissures and ultimately failure or fall off of boards during fires. No insulation materials were studied and only a single heating rate was examined so no conclusions were advanced on expansion and contraction of insulation nor on the impact of rate of heating on contraction in gypsum.

A simpler method for determining volume is to use a caliper to measure linear dimensions, and calculate volume based on the shape of the specimen. Issues arise with this method when considering porous materials where the porosity is unknown, and also if the shape of the specimen is unusual.

A gas pycnometer can be used to determine the volume of various materials regardless of the shape or porosity [46]. One advantage to this method is that it can also be extended to measure the porosity of the material under test. For volume change, the method is analogous to Archimedes' Principle, but instead of a liquid medium it uses pressure measurements in an inert gas medium. The equipment consists of two chambers: a sample chamber and a reference chamber. The volume of each empty chamber must be determined prior to running the experiment. Once a sample is placed in the sample chamber, a valve to that chamber is opened to admit a pressurized gas (usually nitrogen or helium). Once the pressure is equilibrated, the valve allowing pressurized gas to enter the chamber is closed, and the pressure of the sample chamber is noted (P_1). A valve that connects the sample chamber to the reference chamber is then opened, gas pressure

is equilibrated, and the pressure in the reference chamber is noted as P_2 . The volume of the sample can be calculated as shown by [47] using the following equation:

$$V_s = V_c + \frac{V_r}{1 - \frac{P_1}{P_2}} \quad (2.1)$$

with V_s being the sample volume, V_c is the volume of the empty sample chamber, and V_r is the volume of the reference chamber.

This method could be used to measure volume of samples of materials before and after fire exposure to gain insight into volume changes on heating. Currently, this method is not widely used in the area of fire research but it would be useful in determining volumes and volume fraction porosity (see below) of irregularly shaped materials, such as those deformed as a result of being exposed to fire, and those with a porous interior structure as is the case for many insulation materials. ASTM outlines various test standards based on this method. These are typically used in industry for determining skeletal density/volume for materials such as metal powder [48], asphalt binder [49], and plastics [50].

An extension to measurements of volume changes of materials under heating is to also examine the volume fraction porosity. The volume fraction porosity of a material is defined as the fraction of void space relative to the total bulk volume of the sample [51]. Multiple techniques for characterizing the porosity of a material exist, including a variety of microscopy techniques as well as gas and liquid pycnometry methods [52]. Gas pycnometry can be extended to determine the porosity of a material if the user has a means of determining the bulk volume of the material of interest such as [53], which uses this method as a non-destructive way to measure porosity of irregularly shaped meteorites.

2.3.4 Specific Heat Capacity

Specific heat capacity (C_p) is the property of a material that describes the amount of heat required in order to increase the temperature of a material. C_p is measured in units of joules per kilogram Kelvin ($\frac{J}{kgK}$) and can be quantified using Differential Scanning

Calorimetry (DSC). DSC is a characterization method that measures, as a function of time, how much heat is required to change the temperature of a material of interest in relation to that required to change the temperature of a known reference material. From the test information, phase transitions of materials can be studied, and heat capacity of a material can be determined as a function of temperature.

DSC is done on a small scale level using powdered specimens and crucibles pictured in Figure 2.2. The configuration of specimens in DSC tests is similar to that of TGA – there even exists equipment to simultaneously run both DSC and TGA tests in the same machine. The temperature range can be adjusted to fit a researcher’s specific interest; in this case, temperatures should be similar to those seen in structure fires, but since these are generally very high temperatures the range is potentially limited by abilities of available equipment. In addition to temperature range, a DSC user has to choose the heating regime, which would include the heating rate, as well as any cooling periods appropriate to a given study. As for TGA discussed above, the heating regime again ideally would mimic the temperatures in a fire, though these are highly variable from fire to fire. Therefore, previous researchers have again employed various strategies in DSC analysis of the thermal response of construction materials. Brief descriptions of the methods and main results, are outlined below.



Figure 2.2: DSC Specimens and Crucibles.

The NRC ran a series of tests to determine the apparent specific heat of construction materials using a DuPont DSC [23,25]. They used specimens of 10mg – 30mg in mass that were conditioned at 40° C for 24 hours before being tested. DSC tests were run in nitrogen as

well as air from ambient temperature up to 700°C at heating rates of 2, 5, 10, and 20°C/min, though only a single heating rate of 5°C/min was used in investigations of insulation materials, including rock fibre, glass fibre, and mineral wool. Specific heats of both new and preheated mineral wool insulation were determined to distinguish any contribution of heat generated through exothermic decomposition of binders in new insulation during heating. For both rock fibre and glass fibre, measured specific heat leveled off at constant maximum values relatively early into the heating process. In contrast, for new mineral wool insulation, specific heat was found to increase up to temperatures of 300 – 350°C, then rapidly decrease until about 470°C after which it rapidly increased again, leveling off at about 600°C. The peak(s) seen across the mid-range of temperatures reflected the energy that is required to raise the temperature of the material. Specific heats for preheated insulation followed a similar profile until temperatures around 350°C, but subsequently there was a much more gradual decrease in value with no sharp increase again until after 650°C, resulting in a much less pronounced peak which occurred at higher temperature. This is consistent with preheating of the insulation to drive off the binder and reduce the quantity of heat generated by the binder that is available to increase the temperature of the material. Reproducibility of results was examined for mineral wool samples. Agreement in trends of the data was found to be reasonable, however, higher variability of measured values was observed at temperatures higher than 600°C. Such differences were attributed to the differences in composition of the insulations tested.

Sjostrom and Jansson looked at combined TGA and DSC measurements on a STA F3 Jupiter from Netzsch [38]. They tested stone wool fibreboard of density 170 kg/m³ in a nitrogen environment as well as in air by heating the specimen in air from room temperature to 700°C, then cooling and reheating again to 1050°C to explore non-reversible chemical changes induced by heat. In this way, specimens were prepared such that the measurement was free from effects of burning binder and high temperature crystallization processes. DSC traces obtained using new insulation in nitrogen showed several peaks which the authors attributed to exothermal processes that corresponded to vapourization of the binder and glass transitions of amorphous fibre material. Complementary analysis in a 20% oxygen environment, provided estimates for heats of reaction of the binder which

were further used in a simplified model to predict overall behaviour of a larger mineral wool slab under thermal exposure. Finally, reheated samples were analyzed to generate a plot of temperature dependent specific heat without the effects of the above noted exothermal processes. Overall the results were in the same range, but somewhat higher than other results from other mineral wool samples [38, 54].

While studying the thermal properties of gypsum board, [41] determined heat capacity of multiple types of gypsum board (Type C, X, F, R) using two different methods. In one, they obtained the volumetric heat capacity from a Hot Disk measurement and used the room temperature density to determine a value of room temperature specific heat on a mass basis. In order to obtain temperature dependent values of specific heat, they followed ASTM E 1269-2001 [55] to perform DSC analysis on specimens of mass between 6 – 10mg, at a heating rate of 20°C/min in a nitrogen environment. A comparison between Type X and Type R gypsum board, and also between Type C and Type F gypsum board showed specific heat peaks of similar magnitude in DSC results. [41] compared their Type X DSC results to those from [56] and determined that [56]’s results only showed the first of the two dehydration reactions observed in [41], and that [56]’s overall results were slightly higher than reported values in [41]. Again, although no analysis was performed on insulation materials, their comparison of results further supports the use of DSC for determination of temperature dependent values of specific heat capacity in construction materials.

2.3.5 Emissivity

Emissivity is a material property that describes the ability of a material to emit energy as thermal radiation. As such, it is an important parameter in assessment of radiation transfer between materials and their environment in fire situations. ASTM E408 outlines three standard techniques for determining the total normal emittance of surfaces [57]. Test method A is a reflectance method in which radiant energy reflected from the specimen is measured, where Test method B measures radiant energy emitted from the specimen. Test method C measures the near-normal spectral reflectance, that is the radiant energy reflected from the specimen is recorded as a function of wavelength, and converted to a

value of total near-normal emittance.

The reflectance method (Method A) uses the fact that the values for reflectance (ρ), transmittance (T), and absorptance (α) sum to one. Assuming that a material is opaque (i.e., transmittance is zero) and employing Kirchhoff's Law (similar angular and spectral regions) the absorptance is equal to emittance, ϵ , $\alpha = \epsilon$, we can write the following expression:

$$\rho + \epsilon = 1 \tag{2.2}$$

By isolating ϵ and measuring ρ , emittance can be calculated. For this to be strictly valid, the spectral range must equal that of a blackbody at the temperature of the measurement. Therefore, the optical system must be able to take measurements of the reflectance over a complete hemisphere, and the spectral response of the instrument must match closely with the radiance of a blackbody at the temperatures of interest. In order to use Test Method B as outlined in [57], radiant energy emitted and reflected from the specimen passes through a suitable transmitting vacuum window and the radiant heat is measured by a thermopile. From the output of the thermopile a relative emittance reading is given, which must be calibrated with standards of known emittance in order to estimate the value for the test sample.

Test Method C uses a Fourier Transform Infrared Reflectometer (FTIR) to determine the total emittance of samples. A Surface Optics Corporation (SOC) 400T FTIR reflectometer is pictured in Figure 2.3.



Figure 2.3: Emissivity Testing Equipment.

Spectral measurements are taken between 2 and 25 micrometers from a full hemisphere above the sample. The calculation used to find emittance from reflectance is as follows:

$$\epsilon_N = 1 - \frac{\int_0^\infty L_b(\lambda, T) \rho_N(\lambda) d\lambda}{\int_0^\infty L_b(\lambda, T) d\lambda} = 1 - \rho_N \quad (2.3)$$

This method has been used for materials research in the context of determination of emissivity of fabrics [58] as well as materials design and engineering for spacecraft [59]. Although determination of emissivity is important in modeling of thermal response of materials in fire, there are a dearth of references to the use of any of the above methods in the literature for application in materials characterization for fire research.

2.3.6 Thermal conductivity

Thermal conductivity is the property of a material that describes its ability to conduct heat. As such, it is a critical parameter that is used to help estimate heat transfer through materials under exposure to fire [38].

Researchers at the NRC determined time varying thermal conductivity of mineral wool and glass wool insulation using a TC-31 thermal conductivity meter made by Kyoto Elec-

tronics [23, 25]. The meter employs steady-state methods to provide values for thermal conductivity at discrete temperature values [23, 25]. Measurements were obtained over the temperature range between 20°C and 1100°C on specimens that were conditioned at 40°C for 24 hours before testing. Results indicated a gradual, approximately linear, increase in the thermal conductivity of mineral wool insulation with temperature, with some variation in values due to differences in composition of the fibers from sample to sample. In contrast, the conductivity of glass fiber insulation initially increased in a similar fashion, but underwent a sudden increase in value as the glass fibers melted. No comparison of other results from the literature was provided by the authors.

Thermal conductivity was determined by a TPS 2500 – Hotdisk by [38] on mineral wool materials cut into 45 x 100 x 100 mm blocks. A thin probe, made of nickel foil etched into a double spiral pattern with a thickness of 10 μ m was sandwiched between the specimens. For temperatures under 230°C a 25 μ m thick kapton layer was used, and for temperatures between 230°C – 730°C a 60 μ m thick mica cover was used. This setup was placed in an electric furnace in order to measure the thermal conductivity. They curve-fit their results using a second order polynomial and found it to be in line with previous high temperature measurements on stone wool materials of different densities [60].

Nagy et al. studied mineral wool samples to determine whether there was a correlation between the product’s thermal conductivity, moisture content and density of test specimens at approximately room temperature. Using sample sizes between 100 mm \times 100 mm to 300 mm \times 300 mm, they measured thermal conductivity over an area of 50mm \times 50mm using the guarded hot plate method (Taurus TLP 300 DTX) [61]. They found that the thermal conductivity correlated with density and moisture content, however, they did not extend their research to explore high temperature values for the thermal conductivity of their specimens.

In other work, laser flash analysis has been employed to determine thermal diffusivity, heat capacity, and thermal conductivity of materials [62, 63, 64]. This method uses laser pulses directed at the front surface of a specimen and a temperature device on the back of the specimen. The shape of the resulting temperature versus time curve gives the thermal diffusivity, while heat capacity is estimated by determination of the maximum temperature

measured on the rear of the specimen, and the thermal conductivity is calculated using the product of heat capacity and the previously determined density of the specimen [65]. Time-dependent properties are determined by incorporating a furnace into the experimental setup [66]. While this method may show promise for use in determination of materials properties for fire research, no reference to the use of the method for this purpose was found in literature.

Based on the heat transfer models used, and discussion of the literature related to characterization of materials properties important in fire applications, measurements of mass loss, porosity, specific heat, thermal conductivity, and emissivity were identified as most important parameters on which to build a foundation for future development and modelling of the two insulation materials of interest here.

Chapter 3

Methodology

As a first step in the study of the insulation materials, a series of tests designed to mimic the ASTM E136 standard test method for combustibility were completed at multiple tube furnace temperatures. Following this, a series of more detailed materials characterization tests were carried out. Thermogravimetric analysis (TGA) was conducted at various heating rates to gain insight into mass loss of the materials as functions of temperature. From this, the temperature-evolved density of the materials was also deduced. Differential scanning calorimetry (DSC) was then used to measure the specific heat of the materials. Both TGA and DSC were carried out in inert atmospheres to study properties during pyrolysis of the materials, as well as in air to better understand the characteristics of each material when heated in an oxidizing atmosphere such as would be encountered during a fire. These were complemented with experiments targeted explicitly towards measuring other important properties of each material. The emissivity of the materials was characterized through measurements of normal emittance and the skeletal volume (porosity) was measured using the method of Archimedes. Larger specimens of the materials were exposed to constant incident heat flux to investigate heat conduction through, and estimate values for bulk thermal conductivity of, each material, as well as to investigate mass loss on a larger scale than that utilized in the TGA tests. Key parameters and specific measurement methods utilized in the present research for each of these determinations are summarized in the

following sections.

As a final step and preliminary assessment of the approach adopted here, the combined properties from the materials characterization are used as input to a 2-D axisymmetric model to simulate the heat transfer in the large tests. Comparison between predictions and experimentally determined results guides conclusions and recommendations for how small scale data should be collected and used in future models to gain enhanced insight into the behaviour of materials or assemblies during a range of different fire scenarios.

3.1 Materials

The focus of this research is on ROCKWOOL[®] insulation materials. These materials are composed of rock and slag that were melted and spun into fibres which are then held together with an organic cured urea extended phenolic formaldehyde (CUEPF) binder. The specific mineral wool products that form the focus of this research are ROCKWOOL ComfortBatt[®] which has a reported density of 32 kg/m³ [67], and the much denser ROCKWOOL Safe[®] which has a reported density of 72 kg/m³ [68]. Both products are composed of 94-99% mineral fibre, which are reported to have melting points of approximately 1177°C [69], and 1-6% CUEPF binder [70]. A study carried out to characterize the CUEPF binder reported that when the binder alone is heated up to 600°C, a binder mass loss of approximately 80% occurs [71].

3.2 Temperature Measurement

It is very important in the present research to obtain accurate measurements of the temperature of each test material under various heat exposures. Since materials were to be tested up to temperatures commonly encountered in fires, values up to 1000°C needed to be measured. Based on methods used in previous work as well as availability of equipment, thermocouples as well as infrared imaging were chosen. Specifically, K-type thermocouples were used because they are inexpensive, relatively robust, and can measure across the wide

temperature range from room temperature to maximum temperatures of approximately 1260°C [72]. The infrared camera used in this research was a FLIR T650sc IR Camera, which is calibrated to measure temperatures between -40°C – 2000°C across several set ranges and has a detector spatial resolution of 640 pixels × 512 pixels [73].

3.3 Furnace Testing

As an initial step in this research, the thermal response of small samples of the stone wool insulation was investigated by heating small cubic samples across a temperature range of 250 through 750°C in two different furnace configurations. In one set of experiments, samples were heated under similar conditions as those used for the ASTM E136 test [2]. Additional tests, designed to further investigate shrinkage and interior degradation of the insulation samples, were conducted in a larger furnace using cubic specimens. The total mass loss, as well as volumetric change (shrinkage) of each specimen were investigated as described in more detail in the following sections. The resulting data provided information to support creation of multi-physics models of heat and mass transfer through the materials.



(a) Tube furnace specimen.

(b) Cubic furnace specimen.

Figure 3.1: Images of test specimens before being placed in furnace.

As noted above, the first series of heating tests were designed to mimic the ASTM E136

test procedure with modifications due to the availability of equipment in the University of Waterloo. The ASTM method specifies testing $38\text{mm} \times 38\text{mm} \times 51\text{mm}$ samples in a vertical tube furnace consisting of two concentric, refractory tubes, 76 and 102 mm in inside diameter and 210 to 250 mm in length, with heat applied by electric heating coils outside of the larger tube [2]. For the present experiments, the ASTM E136 test was simulated using a horizontal tube furnace readily available at the University of Waterloo, and shown in Figure 3.2. Since the available furnace dimensions were only approximately 4 cm, the specimen dimensions were modified from the ASTM specification as well. Rectangular specimens measuring $5\text{cm} \times 3\text{cm} \times 3\text{cm}$ were cut from the mineral wool insulation and, as illustrated in Figure 3.1a, the corners of the specimens were trimmed down to facilitate insertion into the cylindrical tube furnace. Specimens were prepared and conditioned according to ASTM E136: dried at $60 \pm 3^\circ\text{C}$ for between 24 – 48 hours and placed in a desiccator for a minimum of one hour before testing. Each specimen was then placed in the furnace and exposed to temperatures ranging from 250°C to 750°C , for durations of time between 10 and 30 minutes. Throughout each test, two K-type thermocouples, with 1.59mm bead diameter, were used to record the centre and surface temperatures of the specimen to generate results similar to those that would be expected in the ASTM E136 test. The mass of each specimen was also recorded before and after each test.

A total of 18 tube furnace tests were carried out using furnace temperatures ranging from $250 - 750^\circ\text{C}$. Initially, three tests were carried out for each type of insulation at each of 250, 500, and 750°C . Observations led to the decision to refine the investigation to include tests at 325, 375, 425, and 550°C , so a further two tests were conducted at each of these temperatures as well. One additional test was done at 625°C .

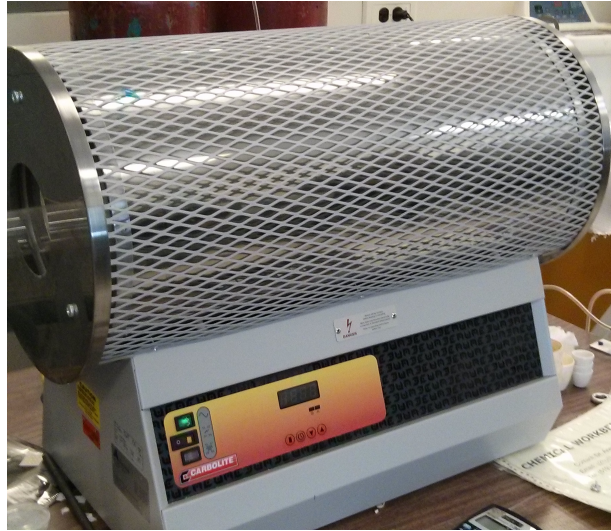


Figure 3.2: Tube Furnace.

In a subsequent series of furnace tests, larger, cubic specimens (Figure 3.1b) were heated to further explore interior degradation and shrinkage of the two materials under heating. Multiple specimens of each insulation type were cut into cubes with side lengths of 5 cm; each side was measured using calipers in order to compare the overall volumetric dimensions before and after heating. Specimens were then placed in a furnace and heated at temperatures of 500°C and 750°C. At each temperature, one specimen was exposed for 10 minutes, another for 20 minutes, and a third specimen was exposed for 30 minutes. After the prescribed time in the furnace, the specimen was removed, and the side lengths were measured again using the calipers. From this data, the volume change was calculated. Afterwards, each specimen was cut in half and any interior degradation was assessed visually.

3.3.1 Calculations

Once the data from the furnace tests had been collected, the results were compared to the criteria for combustibility specified in the ASTM E136 standard test method [2]. A material is considered to be non-combustible according to ASTM E136 if the mass loss of the specimen is 50% or less, the centre temperature of the specimen does not rise more

than 30°C higher than the stabilized furnace temperature during the 30 minute heating period, and there is no flaming from the test specimen after the first 30 seconds [2]. A material can also pass the test if the mass loss is more than 50%, as long as the surface or centre temperature of the specimen does not rise above the stabilized furnace temperature, and there is no flaming.

For each test, therefore, the measured centreline temperature of each sample was compared to the furnace temperature, and the percent mass loss was calculated after 30 minutes of exposure using Equation 3.1.

$$dm\% = \frac{m_0 - m_1}{m_0} \times 100. \quad (3.1)$$

For the larger samples in the furnace tests, the volume of the samples were calculated by using:

$$V = x_1 \times x_2 \times x_3 \quad (3.2)$$

Where x_1 , x_2 , and x_3 are the linear dimensions of the sample. The change in volume was calculated using:

$$dV = V_0 - V_1 \quad (3.3)$$

Where V_0 and V_1 are the initial and final volumes of the specimen, respectively.

3.3.2 Porosity

As an extension to the above furnace heating studies, the skeletal volume (porosity) of the insulation samples was measured to study bulk volume change as well to explore changes in porosity that occur due to possible thermal decomposition, material degradation and/or cavitation as the mineral wool insulation samples were exposed to heat. The results were intended as input to simple one dimensional conduction models that have been used

successfully in the past to model heat transfer through porous materials, where for the case of this research the fluid in the material pores is air [74].

In these tests, therefore, the porosity of each of the mineral wool insulation materials was determined using Archimedes' Principle of water displacement. This method was time and cost effective and required very little specialized equipment. Cuboids of each type of insulation were cut, and the bulk volume was calculated from the measured dimensions using Equation 3.2.

Bulk density of the material was calculated by dividing the measured mass of each cuboid by the bulk volume:

$$\rho = \frac{m}{V}. \quad (3.4)$$

The specimen was then placed in a known volume of water, compressed to remove any air pockets, and the volume of water displaced was recorded as the skeletal volume of the material. The porosity (void fraction) was calculated by dividing the pore volume, which was calculated as the difference between the bulk and skeletal volume, by the bulk volume:

$$\phi = \frac{V_B - V_{sk}}{V_B}. \quad (3.5)$$

3.4 Characterization Experiments

Following the furnace tests above, a series of more detailed materials characterization tests were carried out. In the first stage of characterization, thermogravimetric analysis (TGA) was conducted at heating rates of 2, 5, and 10°C/min to further investigate mass loss of the two insulation types as functions of temperature, thereby deducing the temperature-evolved density of the materials. Differential scanning calorimetry (DSC) was used to measure the specific heat of the materials. Both TGA and DSC were done in inert atmospheres and in air to better understand the characteristics of each insulation when heated in pyrolyzing or oxidizing atmospheres such as would potentially be encountered during different phases of

a fire. Finally, larger specimens of the materials were exposed to a constant incident heat flux to investigate heat conduction through each material, and mass loss on a larger scale than TGA. These tests are described in more detail in each of the following few sections.

3.4.1 Thermogravimetric Analysis

The TGA tests were carried out using a TA Instruments Q500 TGA apparatus that was available at the University of Waterloo [75]. Before testing, samples of each material were powdered using a mortar and pestle and the powdered materials were allowed to equilibrate to lab conditions for a minimum of 24 hours. Immediately before testing, a 10 mg specimen was placed in a TGA sample tray, as seen in Figure 3.3. The sample mass chosen is similar to that used throughout the literature [23,25]. During the analysis, the mass of each individual specimen was measured as it was heated in air, from ambient to 800°C, at heating rates of 2, 5, and 10°C/min, respectively. Additional samples were heated in nitrogen at a single heating rate of 5°C/min. The heating rates chosen here matched those in the literature that were found to produce consistent data during thermal degradation studies of construction materials [23,25,38]. The upper temperature limit of 800°C, while slightly lower than the value used in other studies [23,25,38] was driven by the equipment available for conduct of the tests. The weight precision of the TA Q500 was $\pm 0.01\%$ and isothermal temperature accuracy and precision were $\pm 1^\circ\text{C}$ and $\pm 0.1^\circ\text{C}$, respectively. In these studies, mass change during heating is the primary measurement, and the rate of mass change is computed numerically using the TA Universal Analysis software v5.5.24 [75].



Figure 3.3: TGA Testing Equipment.

3.4.2 Specific Heat Capacity

A NETZSCH DSC 404 C, available at the University of Waterloo, was used for measurement of temperature dependent specific heat of the mineral wool insulation samples. The temperature and heat flow calibration followed ASTM E967 [76] and ASTM E968 [77] methods, respectively. Test parameters again were chosen based on those previously reported in DSC analysis of insulation materials in the literature [23,38]. A mortar and pestle was again used to powder specimens of each material which were allowed to equilibrate to lab conditions for a minimum duration of 24 hours. The heat flow into or out of small samples of insulation, approximately 10mg each, were determined in the DSC 404C under a heating rate of 10°C/min across the temperature range from 30-1200°C in air and an inert (argon) environment. Heat flow data was recorded as a function of temperature and the ASTM E1269 method was used for determining specific heat capacity [55]. When considered alongside Differential Scanning Calorimetry (DSC) data from a sapphire standard, the specific heat capacity of the test specimen was calculated according to Equation 3.6:

$$C_{p,s} = C_{p,st} \frac{D_s W_{st}}{D_{st} W_s} , \quad (3.6)$$

where C_p is the specific heat capacity, D is the vertical displacement measurement measured

from a DSC thermal curve of temperature versus time, and W is the mass of sample that corresponds to a given time. The subscripts s and st refer to the test specimen and the sapphire standard respectively.

In the next stage of more detailed characterization of the thermal properties of the two mineral wool insulation samples, the TGA and DSC tests outlined above were complemented with experiments targeted explicitly towards measuring other important properties of each material as described in the following two sections. The first described measurements focused towards determining the emissivity of the two insulation materials. In the second, larger specimens were exposed to constant incident heat flux to investigate mass loss on a larger scale than in the TGA tests, as well as to investigate heat conduction through, and estimate values for bulk thermal conductivity of, each material.

3.4.3 Emissivity

In these tests, estimates of surface emissivity of each of the insulation types were determined using a Surface Optics Corporation (SOC) 400T FTIR available at University of Waterloo according to Method C in ASTM E408 1319 [57] and described in detail in Section 2.3.5. Bulk samples of each insulation were conditioned prior to testing for a minimum of 24 hours to approximately 20°C and 30% relative humidity. The SOC 400T FTIR reflectometer was used to measure the wavelength dependent reflectance of each material based on room temperature thermal radiation. The reflectivity of the samples were determined by comparing measured values to values obtained using a NIST Traceable reference standard. The total near-normal emittance (equal to the near-IR absorptance for opaque samples) of the sample was calculated by subtracting the measured IR reflectance from 100%. As a final step, emissivity was calculated as a function of temperature using a linear estimation by the equipment software according to the method in Section 2.3.5. Measurements of room temperature reflectance from this apparatus are accurate to $\pm 1\%$.

3.4.4 Thermal Conductivity

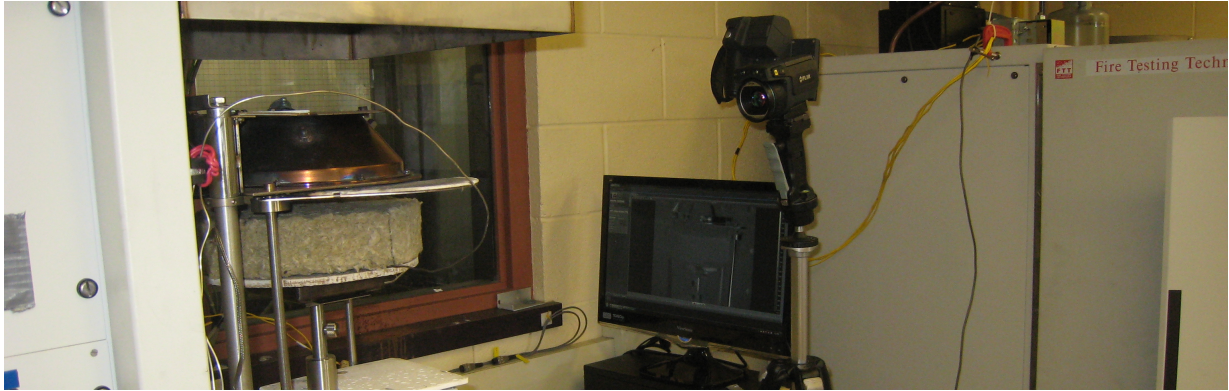


Figure 3.4: Cone Calorimeter Thermalconductivity Test Setup.

A heat transfer experiment was designed and carried out to determine the thermal conductivity out of the insulation materials using a cone calorimeter heating element and load cell (Figure 3.4). The objective was to gain additional insight into thermal response and heat penetration of large specimens of each insulation. Further, the data was intended to couple with a model that would allow the back-calculation of values for thermal conductivity of the materials.

The experiments used disc-shaped specimens, 230 mm in diameter and between 54 and 56 mm thick, cut from slabs of insulation and conditioned in the lab for 24 hours or more. Each disc was mounted on a 230 mm diameter disc of 7.7 mm thick concrete board, and placed on the load cell of the cone calorimeter and exposed to a constant incident heat flux of 25, 35, or 50 kW/m² for a minimum duration of one hour or until measured temperatures approached steady state values. Throughout each test, mass loss of the specimen during heating was recorded via the cone calorimeter load cell. The temperature of the unexposed side of the specimen was measured via two thermocouples affixed to the top of the concrete board (under the specimen) at radial positions of $r = 0$ (the centreline) and $r = 70$ mm. An additional thermocouple was placed on the edge of the specimen, at a position 27 mm below the top surface, to gauge the level of heat loss through the side of each sample. Sample

surface temperatures were monitored using a FLIR infrared camera at measurement points chosen to correspond to the thermocouple mounting locations on the unexposed side ($r = 0$ and $r = 70$ mm), illustrated in Figures 3.5, 3.6 and Table 3.1. Two tests were conducted on each sample: in the first, the conditioned virgin specimen (never exposed to heat) was exposed to the given level of incident heat flux; in the second, the same specimen was exposed to the same heat flux for a second time using the same methodology to ascertain potential changes in thermal properties of a previously heat exposed sample.

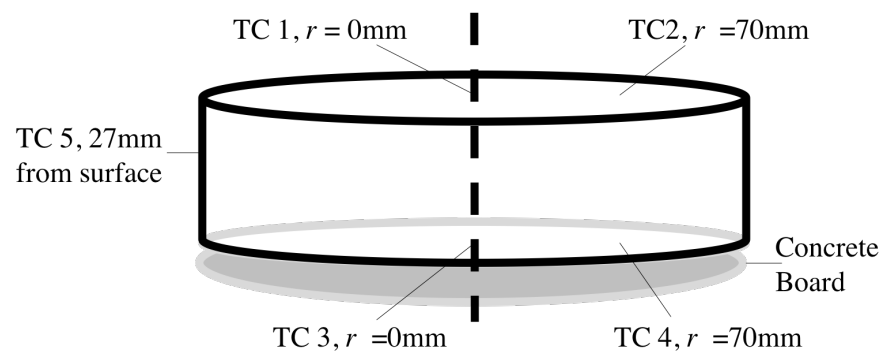


Figure 3.5: Thermocouple Placement

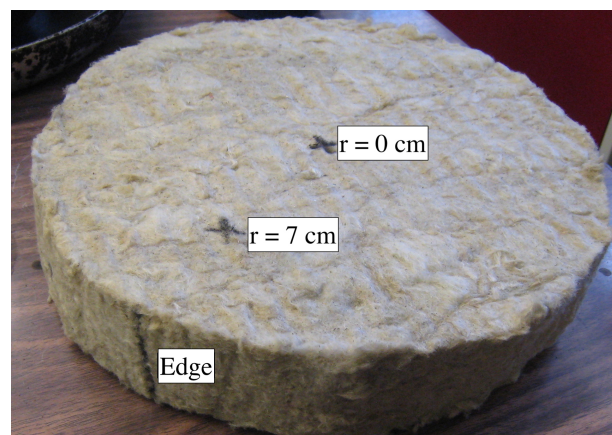


Figure 3.6: Specimen

Table 3.1: Thermocouple Numbering

Thermocouple	T1	T2	T3	T4	T5
Location	$r=0$, Top	$r=70\text{mm}$, Top	$r=0$, Bottom	$r=70\text{mm}$, Bottom	Edge

3.5 Two-Dimensional Axi-Symmetric Model

There are many aspects to consider when modelling heat transfer through materials across the wide temperature ranges characteristic of those encountered during fires. The material properties and how they change under exposure to heat, as well as the surrounding ambient conditions, have a significant impact on the behavior of a material. Yet, these details can be difficult to reflect accurately when creating a simulation. This challenge in part motivated the creation of a two-dimensional axisymmetric model developed with the goal of predicting the temperature profiles within specimens exposed to irradiance from a cone calorimeter [78], [79]. It is used in this work to predict the results of the experiment outlined above on the thermal transfer through cylindrical “slabs” of insulation material under specified heating conditions [78], [79].

The model was previously verified [78], [79] using a test case of heat transfer through a steel slab under heat exposures of 25 and 50 kW/m², cross-checked against temperature measurements collected at specified locations. The predictions were found to be in good agreement with the experimental results prompting use of the model in this research as well. The model requires parameters for specific heat, thermal conductivity, emissivity, and density. These were either obtained from the literature or based on results of the material’s characterization experiments outlined above.

The model is an explicit finite difference scheme that uses the energy balance method with the resultant equation being a combination of the conservation of energy and Fourier’s Law of conduction. The one and two dimensional formulations are shown in Equations 3.7 and 3.8, respectively.

$$\rho c_p \frac{\partial T}{\partial t} = \frac{\partial}{\partial z} \left(k \frac{\partial T}{\partial z} \right); \quad (3.7)$$

$$\rho c_p \frac{\partial T}{\partial t} = \frac{1}{r} \frac{\partial}{\partial r} \left(kr \frac{\partial T}{\partial r} \right) + \frac{\partial}{\partial z} \left(k \frac{\partial T}{\partial z} \right). \quad (3.8)$$

Heat transfer through the specimen itself is modelled; boundary conditions are specified to account for the ambient surroundings and to replicate the operating characteristics of the cone calorimeter used as the heat source in the experiments. The cone heater is assumed to be an ideal or black body emitter ($\varepsilon = 1$), and the boundary condition for the exposed surface (A) is given by:

$$\left. \frac{\partial T}{\partial z} \right|_{z=0} = \frac{\varepsilon_A}{k_A} q_e'' - \frac{\varepsilon_A \sigma}{k_A} (T_s^4 - T_\infty^4) - \frac{h_{c,top}}{k_A} (T_s - T_g), \quad (3.9)$$

where q_e'' is radiative heat flux from the cone, k represents thermal conductivity of the specimen material, σ represents the Stefan-Boltzmann constant, and h is the convection heat transfer coefficient for the top surface. The view factor between the cone heater and the surface of the specimen is inside of the first term, as this is a measured value. All aspects outlined in [78], [79] regarding the cone calorimeter were kept the same because this experiment used the same configuration and same equipment as in earlier experiments. The model is discussed in detail in [78].

The model assumes that the bottom surface of the sample, in this case concrete board, is completely open; contact with the load cell platform is neglected. The sides of every layer are exposed to ambient conditions of the surroundings which are assumed to remain at the same temperature for the duration of a test. The emissivity and convection coefficient depend on the material properties and physical dimensions of top and bottom layers, respectively. The material properties used in the model are outlined in Table 4.6, and the convection heat transfer coefficient uses the same method as outlined in [78], which is calculated as a function of temperature for the top, side, and bottom surfaces separately. The boundary conditions used in [78], [79] are summarized below.

Exposed surface

The exposed surface boundary condition accounts for radiation from the cone heater to the specimen surface, as well as convection and radiation from the specimen surface to ambient surroundings. Note that A denotes the top material in the model, in the present case, ROCKWOOL Safe[®] insulation. T_g is the hot gas temperature near the centreline, which was determined in [78], [79]. q_e'' is the radiative heat flux from the cone heater.

$$\left. \frac{\partial T}{\partial z} \right|_{z=0} = \frac{\varepsilon_A}{k_A} q_e'' - \frac{\varepsilon_A \sigma}{k_A} (T_s^4 - T_\infty^4) - \frac{h_{c,top}}{k_A} (T_s - T_g), \quad (3.10)$$

Unexposed surface

The unexposed surface assumes that the bottom surface (concrete board) is completely open, neglecting contact with the load cell and accounts for radiative and convective heat transfer. Note that C denotes the concrete board layer.

$$\left. \frac{\partial T}{\partial z} \right|_{z=L} = -\frac{\varepsilon_C \sigma}{k_C} (T_s^4 - T_\infty^4) - \frac{h_{c,bot}}{k_C} (T_s - T_\infty). \quad (3.11)$$

Side surface

The side of the specimen and the concrete board are exposed to ambient. i represents the material (insulation or concrete board) and this boundary condition accounts again for radiative and convective heat transfer.

$$\left. \frac{\partial T}{\partial r} \right|_{r=R} = -\frac{\varepsilon_i \sigma}{k_i} (T_s^4 - T_\infty^4) - \frac{h_{c,side}}{k_i} (T_s - T_\infty), \quad (3.12)$$

Chapter 4

Results and Discussion

4.1 Furnace Testing

4.1.1 ASTM E136 Test Results

The percent mass loss of the ROCKWOOL Safe[®] insulation as a function of exposure temperature is illustrated in Figure 4.1, as calculated using Equation 3.1. As expected, the mass loss increased with exposure temperature, starting at 1% at 250°C and stabilizing at 4% for furnace temperatures above 550°C. As these values are well below the 50% mass loss criteria that is specified as the pass/fail criterion in ASTM E136, this part of the combustibility test is easily satisfied. More importantly from the point of view of understanding the thermal characteristics of the material, the measured values of mass loss are consistent with what might be expected. It was reported by Poljanšek [71] that a similar binder to that used in the mineral wool insulation samples here loses approximately 80% of its mass by the time it is heated to 600°C. The binder content of the insulations is listed as between 1 and 6% by mass [70]. The predicted mass loss of the binder in the present samples, according to the values reported in [71], should then be between 0.8-4.8%. Assuming that the binder is the only significant component that contributes to mass loss, the results are consistent.

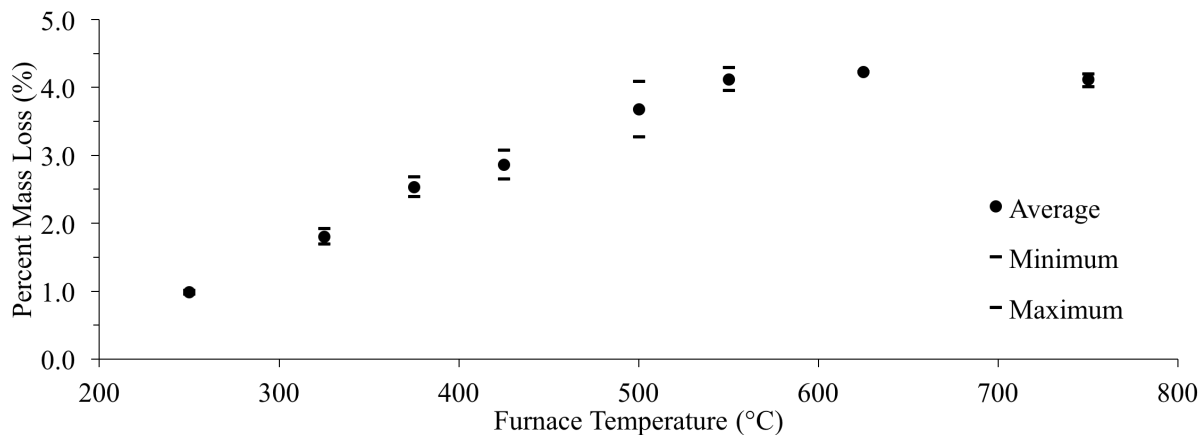


Figure 4.1: Percent mass loss of specimens tested at various furnace temperatures.

Figure 4.2 shows the average centreline and surface temperatures across furnace tests conducted at 250, 500, and 750°C, respectively. During heating with the oven temperatures set at 250 and 750°C, it is apparent that the sample surface temperature first rises rapidly and begins to approach the furnace temperature. At the same time, there is a delay before the centreline temperature begins to rise, and subsequently the centreline temperature rises less rapidly to approach the furnace temperature. In contrast, when the samples are heated with the oven at 500°C the centreline temperature actually increases to a value above the surface temperature of the sample and also exceeds the prescribed furnace temperature by approximately 40°C. Based on the ASTM E136 combustibility criteria that the centreline temperature cannot rise by more than 30°C above the stabilized furnace temperature, the ROCKWOOL® Safe insulation material would appear to fail the temperature requirements of the ASTM E136 combustibility test when heated in a furnace held at a constant temperature of 500°C, but meet them when heated in a furnace held at the higher temperature of 750°C. This is likely an indication of exothermic reaction, and potentially combustion, of the binder in the insulation. When the furnace temperature is at 500°C, the internal temperature increase to values above the furnace exposure temperature is discernible by the thermocouples. Whereas when the furnace temperature is higher, the reactions that occur inside of the insulation do not increase the interior temperature to values above that of the furnace so the effect is much less discernible. Based on this

preliminary finding, it was decided to expand the range of furnace exposure temperatures on the samples, and in particular, to add more testing at temperatures around 500°C. Additional specimens were therefore prepared and tested in the same fashion as the initial set, at furnace temperatures of 325, 375, 425, 550, and 625°C. Results are shown in Figure 4.3 as the difference in average measured temperature between the centreline and surface temperatures for each test.

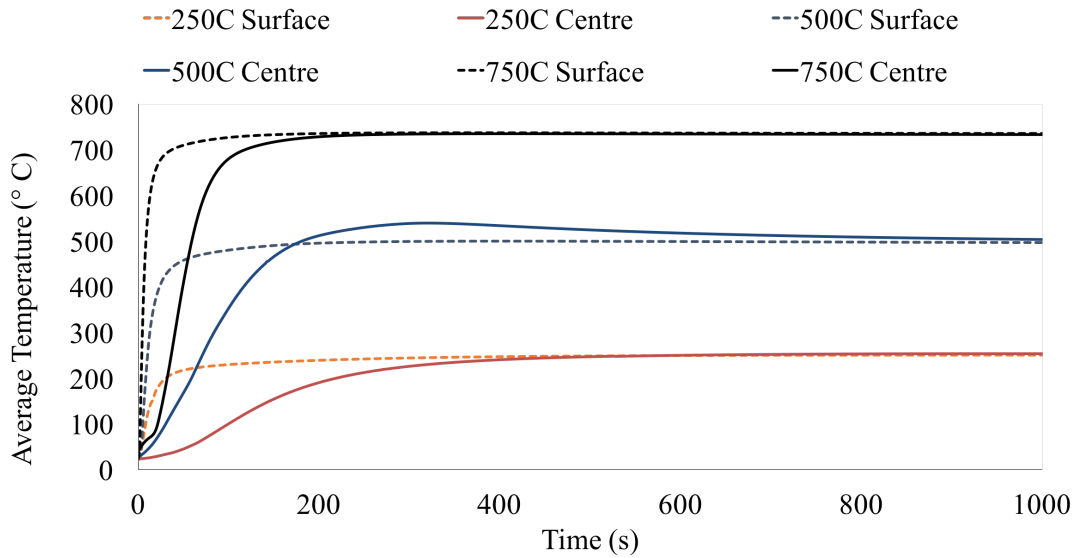
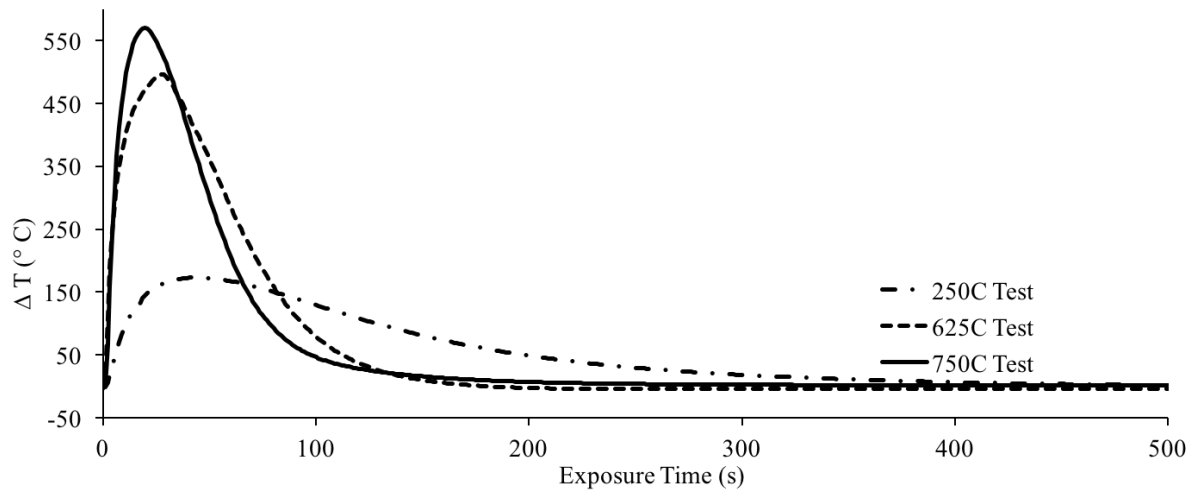


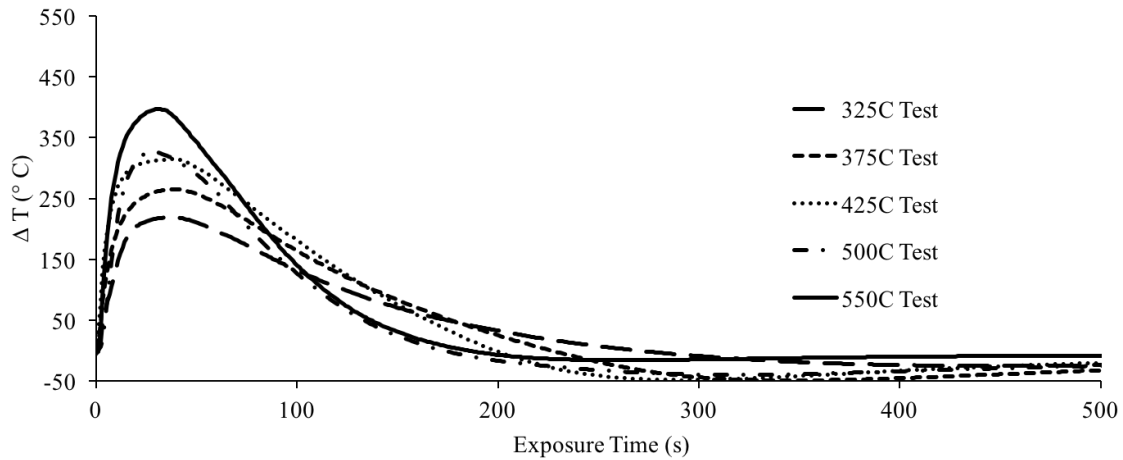
Figure 4.2: Average temperatures of centre and surface throughout a test.

Figure 4.3 illustrates the difference between the average sample surface and interior (centre) temperatures (Equation 4.1) for each furnace exposure using,

$$\Delta T = T_{surface} - T_{centre}. \quad (4.1)$$



(a) Tests where the centreline temperature does not exceed the surface temperature.



(b) Tests where the centreline temperature exceeds the surface temperature.

Figure 4.3: Temperature difference between surface and centre temperatures of specimens at various furnace temperatures.

The figure is split into two parts: Figure 4.3a for exposure temperatures of 250, 625, and 750°C, in which the temperature difference did not fall below zero, and in contrast, Figure 4.3b, for tests at exposure temperatures of 325, 375, 425, 500, and 550°C in which the temperature difference did fall below zero (i.e., the measured interior temperature is hotter

than the furnace temperature). In all cases, the expected initial increase in the temperature difference between the surface and centreline of the sample can be observed. This difference reaches a maximum value within the first 30 seconds, followed by a decrease over time. The surface temperature initially rises rapidly to approach the furnace temperature, while the centre temperature rises at a slower rate but for a longer time than the surface temperature. After the initial peak, the surface and centre temperatures converge for tests conducted at furnace temperatures of 250, 625, and 750°C. The temperature differences for tests conducted at all intermediate furnace exposure temperatures, however, first fall below zero and then converge. The figure clearly shows that the interior temperature of the specimen is hotter than the surface temperature for a period of time, implying that at certain heating rates the material appears to undergo an internal self heating process possibly via exothermic reaction as mentioned above.

4.1.2 Interior Degradation and Shrinkage

To evaluate the hypothesis of self heating in the samples at some temperatures, all of the heated insulation specimens were sectioned and their interiors were examined. The cross sections for a series of tube furnace specimens heated at different furnace temperature are shown in Figure 4.4. There is marked discolouration and/or degradation observed at the centre of all of the sectioned specimens for which measured temperatures were plotted in Figure 4.3b. It is clear that there is more degradation of the specimens in the centre than on the surface, but unclear whether this is an indication of self heating of the material, or an artifact of heat transfer due to a metallic sheathed thermocouple being inserted into the centre of the specimen. To better understand these results, an additional series of tests were conducted on slightly larger specimens without instrumentation (Figure 3.1b) for the purpose of observing both interior degradation as well as measuring total shrinkage of the materials under exposure to heat. In this case, specimens were exposed to temperatures of 500 and 750°C for times of 10, 20, and 30 minutes. Figures 4.5 and 4.6 show the post-exposure condition of the specimens. For the specimens heated at 500°C, it appears that interior degradation is the most severe after 30 minutes of exposure, but signs of

discolouration and density change are present even after 10 minutes, as indicated by the circled regions in Figure 4.5. Qualitatively, there does not appear to be a significant difference between the interior degradation after 10 and 20 minutes of exposure. For exposure in an oven at 750°C, there does not appear to be significant difference between any of the exposure durations – a cavity is evident at the centre of the specimens for all exposures. Consistent with the measurements of mass loss outlined above, it is clear from these results that internal heating and consequent degradation of the insulation is occurring as the samples are heated both at 500 and 750°C.



Figure 4.4: Interior Degradation of Tube Furnace Specimens.

To further explore the impact of interior degradation with respect to the characteristics of the insulation under exposure to heat, the total volumetric change of each specimen was determined for each of the exposure times and temperatures by using Equation 3.2.

Unfortunately, there is insufficient resolution in these measurements to distinguish a trend in the change in volume of the samples with time. Mean shrinkage of insulation specimens exposed to 500°C furnace temperatures is 4%, and for 750°C furnace exposures the mean shrinkage is 31%. This result is consistent with observations from Figure 4.6 of the

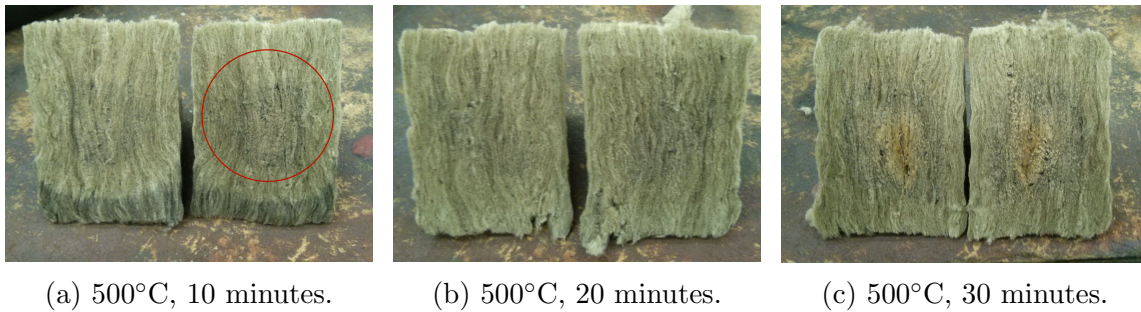


Figure 4.5: Cubic furnace specimens – 500°C for various exposure times.

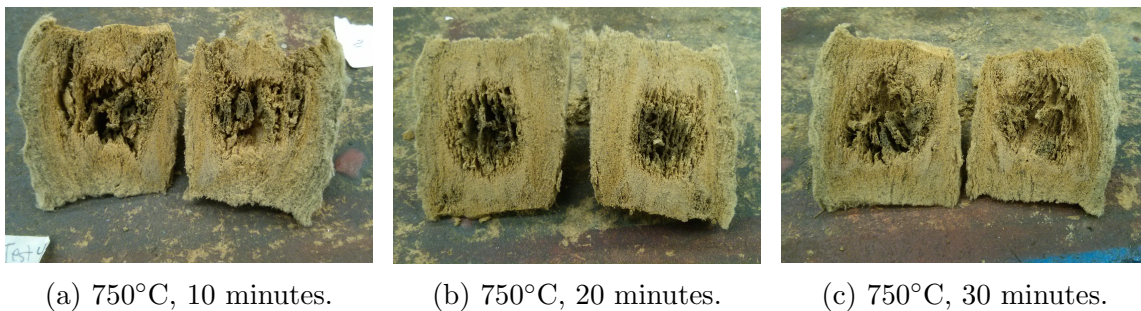


Figure 4.6: Cubic furnace specimens – 750°C for various exposure times.

discoloured cavities in the centre of each specimen and is a clear indication that at increased exposure temperatures the insulation undergoes more degradation and is therefore subject to greater overall volumetric changes.

It is interesting to note that the ROCKWOOL[®] Safe board insulation tested appears to meet the temperature requirements of the ASTM E136 combustibility test at 750°C exposures. In sharp contrast, it appears to fail the test due to internal self heating when exposed to lower temperatures of 500°C. As seen in Figure 4.3a above, at temperatures below 325°C, the centreline temperature does not at any time exceed the surface temperature of the insulation samples tested. There is also no sign of internal degradation under heating at these lower temperatures, with only a slight colour change in the material after the full 30 minute exposure. In contrast, measured centreline temperatures in tests at temperatures between 325°C and 550°C do exceed the temperature of the surface at some point during the test, indicating that at any of these temperatures, the specimens would

fail the ASTM E136 test. Interestingly also, visible signs of internal self heating and degradation are not apparent in insulation samples exposed to furnace temperatures less than 500°C. However, since the temperature difference between the interior and exterior of the samples begins to diverge above 325°C (Figure 4.3b), despite lack of visible evidence, the material still undergoes some thermochemical changes at temperatures lower than 500°C.

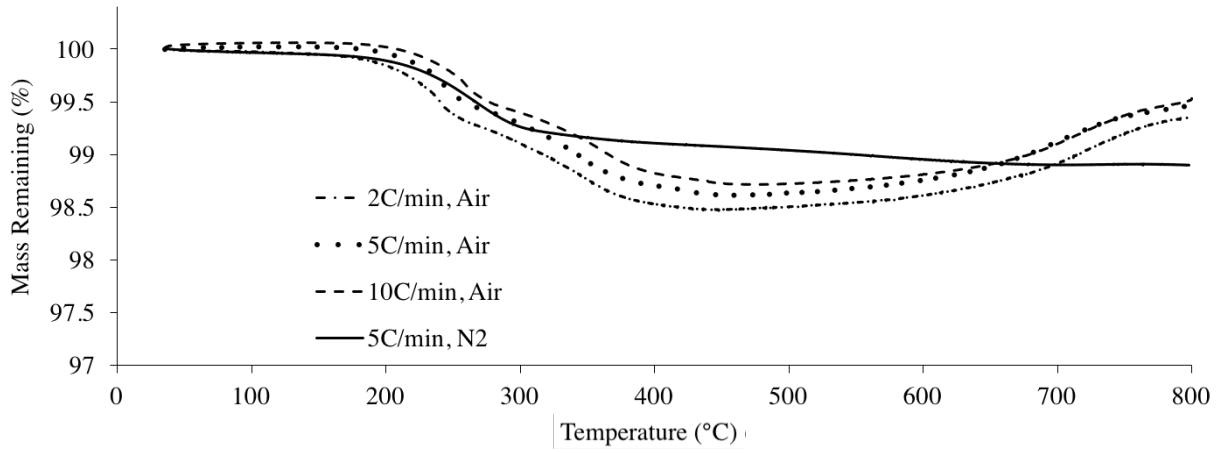
The spherically shaped cavitation seen in the interior of specimens in Figure 4.6 supports that an exothermic reaction involving the binder is occurring, which produces a pressurized volume of hot gas that pushes out isotropically from the centre of the specimen against incoming gas. The process may be similar to that previously observed during manufacturing of materials in which a solid substrate is injected with a binder and then heated for a prolonged period of time in order to burn off the binder and obtain the final product. According to [80], slow heating rates are required when burning off the binders to avoid creation of high internal gas pressures and the potential for the formation of bubbles or cracks and other undesired defects in the material. The rate at which the gas from the binder is produced has been found to be proportional to the heating rate, which in the present study may be why cavitation is less severe at lower temperatures, as illustrated in Figure 4.5. The heating rate at 500°C is low enough that any internal pressure built up as the binder decomposes can equilibrate with atmospheric pressure as the specimen continues to heat. At the higher temperature exposures, the heating rate is most likely faster and increased internal sample pressures due to build up of degradation gases from the binder cannot equilibrate with atmospheric pressure, so the fibres are moved by the forces exerted by the expanding hot gas, thus creating a spherical shaped cavity inside each specimen. As the exposure temperature exceeds about 600°C, significant internal degradation begins to occur, as seen in Figure 4.6, and a large cavity in the centre most likely forms fairly quickly and then fills with gas at approximately the same temperature as the surrounding furnace gases. Thus, even though the material undergoes more significant thermal degradation at furnace temperatures exceeding 600°C, the measured centreline temperatures do not appear to exceed the surface temperatures during the test. In this case as well, the material would no longer be classified as combustible by the ASTM E136 definition.

4.2 Characterization Experiments

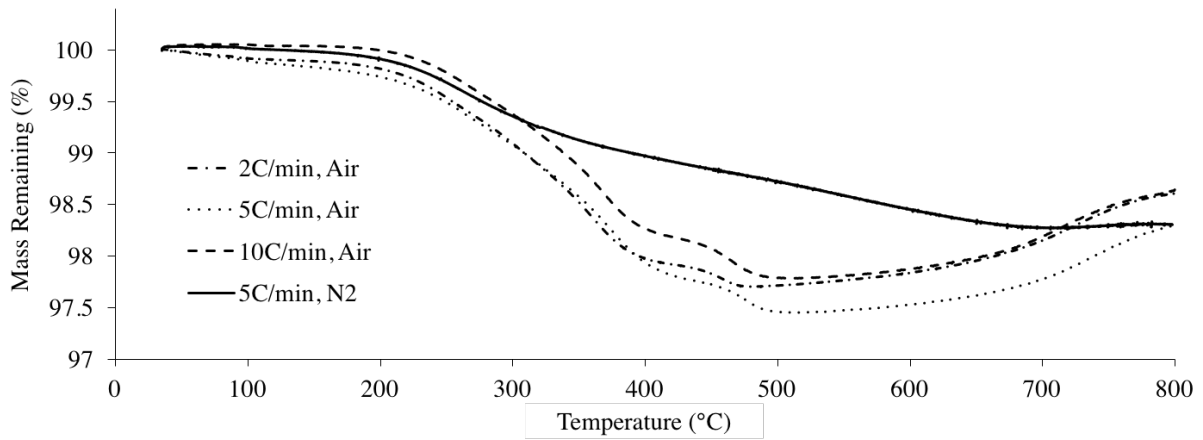
4.2.1 Thermogravimetric Analysis

TGA mass loss curves obtained at 2, 5, and 10°C/min in air and at 5°C/min in a nitrogen environment are illustrated in Figure 4.7. The figure shows that trends in mass loss for a single sample of insulation heated at different rates, as well as between the two types of mineral wool insulation, are very similar. The measured total mass loss changed by only about 0.2% for a given type of insulation across the different heating rates.

The average percent mass loss for each type of insulation, and the average temperatures at which the maximum rate of change of mass relative to temperature occurred, are reported in Table 4.1 for both air and nitrogen tests. The rate of change of mass relative to temperature is at a maximum for temperatures between 250–350°C, which is within the same range as the furnace mass measurements in Figure 4.1, where the maximum rate of change of mass is between 250–500°C. The furnace test results that outline the internal decomposition (Section 4.1) show visible degradation by 500°C, which is consistent with a majority of the mass being lost before that temperature. The average mass loss in nitrogen is only 80% of that in air for both materials, reinforcing the finding that oxygenated pyrolysis does occur in these two insulation samples. Further, the table shows that the temperature at which the maximum value of dm/dT occurred was identical for both materials in nitrogen, but significantly different in air. This would indicate that the two materials undergo similar pyrolysis in the absence of oxygen, but different decomposition and oxidation processes when oxygen is present. Interestingly, the ROCKWOOL ComfortBatt® material had a greater average mass loss in both environments, perhaps indicating that the binder content of this material is greater than the ROCKWOOL Safe® product. In modelling a fire scenario, both threshold temperature for interior decomposition and differences in overall mass loss of the ComfortBatt® versus Safe® insulation may both have to be considered particularly when the details of thermal transfer and materials behaviour is critical in the final predictions.



(a) ROCKWOOL Safe®



(b) ROCKWOOL ComfortBatt®

Figure 4.7: TGA Test Results

Table 4.1: TGA Mass Loss Summary

Material	Average Mass Loss (Air, %)	Average Mass Loss (N ₂ , %)	Temperature of max dm/dT (Air, °C)	Temperature of max dm/dT (N ₂ , °C)
Safe [®]	1.412	1.126	246	264
ComfortBatt [®]	2.284	1.848	368	264

It was reported by Poljanšek [71] that a similar binder to that used in the mineral wool insulation here loses approximately 80% of its mass by the time it is heated to 600°C. The binder content of the two mineral wool materials is listed as between 1-6% by mass [70]. The predicted mass loss of the binder in the present samples, according to the values reported in [71], should then be between 0.8-4.8%. Results from the present TGA in air indicate an average mass loss of 1.412% and 2.284% for Safe[®] and ComfortBatt[®], respectively, and thus fall within the anticipated range. These results are summarized in Table 4.1

The TGA results for specimens in air each show consistent increases in specimen mass beginning at approximately 400–500°C. This phenomena is likely due to an oxidation reaction occurring. This was the likely cause in these results, as this same phenomenon was not observed for tests carried out in the inert environment.

The average onset temperatures for changes in each material as calculated by the TA Universal Analysis software are reported in Table 4.2. The initial onset temperatures are the temperatures at which mass loss begins to occur, which indicates when a material begins to undergo a thermally induced reaction. This temperature is typically used as an indicator of the thermal stability of a material, and any following thermal transitions or “bumps” are indications of other separate thermally induced events. The results presented in Table 4.2 are extremely consistent between the two materials examined here. This is expected due to the similarity in fibres and particularly the binder used in the products.

Table 4.2: Material Event Onset Temperatures

Material	Average Initial Onset Temperature (°C)	Average Secondary Onset Temperature (°C)	Average Tertiary Onset Temperature (°C)	Average Final Onset Temperature (°C)
Safe [®]	223	304	329	421
ComfortBatt [®]	215	303	352	451

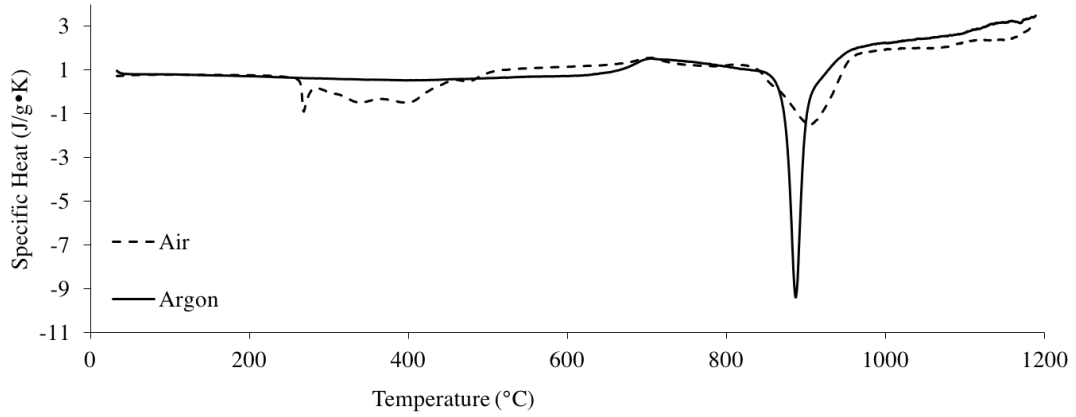
4.2.2 Specific Heat Capacity

DSC results are presented as plots of specific heat capacity as a function of temperature in both air and argon environments (Figure 4.8). The temperatures at which major thermal effects (thermal transitions or chemical reactions) occur are documented in Table 4.3. Comparison of the results in Table 4.3 with those reported in Table 4.2 indicates that the initial onset temperatures of thermally induced changes in properties for both materials in air are consistent between TGA and DSC tests; the agreement is particularly good for the ROCKWOOL Safe[®] material.

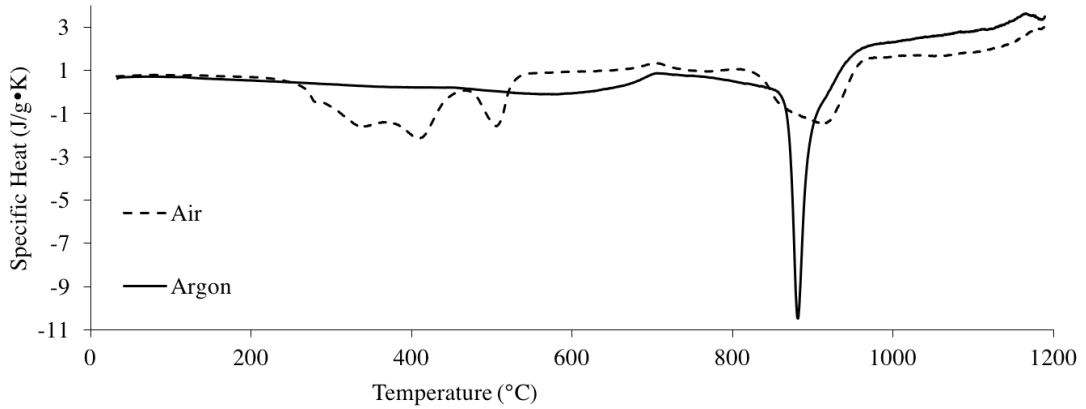
Reactions that are exothermic or endothermic are indicated by peaks in a DSC plot. Exothermic processes can be discerned from endothermic ones by a positive or negative concavity, respectively. Results from the DSC testing highlight that the temperature region with the most activity (multiple exothermic reactions) for exposure of the insulation in air occurs between approximately 200 and 550°C. This is consistent with the other characterization data since it corresponds to the temperature range in which multiple mass loss events occurred (Table 4.2) in the TGA tests, and the temperatures at which the maximum rate of mass loss occurred (Table 4.1). These results are also consistent with the furnace tests in Section 4.1. The significant visible interior degradation occurred during exposures of 500°C and higher, indicating that a majority of the “activity” would have occurred prior to that temperature. Similarly, the maximum rate of mass loss was found to be within the range of the most activity in the DSC data.

Table 4.3: DSC Major Event Temperatures

Material	Initial Onset Temperature (Air, °C)	Initial Onset Temperature (Argon °C)	Second Major Event Temperature (Air, °C)	Second Major Event Temperature (Argon, °C)
Safe [®]	220	650	810	840
ComfortBatt [®]	190	630	805	840



(a) ROCKWOOL Safe[®]



(b) ROCKWOOL ComfortBatt[®]

Figure 4.8: DSC - Specific Heat Results

4.2.3 Porosity

The mean porosity and standard deviation for ROCKWOOL Safe[®] and ROCKWOOL ComfortBatt[®] are 0.961 ± 0.006 and 0.983 ± 0.004 , respectively. All measurements were taken using virgin material which had not been heated. While it would be interesting to determine the change in porosity of the materials after exposure to heat, the present measurement method did not have sufficient resolution to distinguish such differences. The writer was not able to access an alternate method for measuring porosity, such as gas pycnometry, as the equipment was not available.

4.2.4 Emissivity

Emissivity measurements were conducted using the methods outlined in Section 3.4.3 on a variety of commonly used construction materials. Once the materials were prepared, the SOC 400T FTIR was used to measure the wavelength dependent reflectance of each material based on room temperature radiation (293K). Using a NIST traceable reference standard, the reflectivity of the samples were determined, and using the method in Section 3.4.3, the emissivity (total near-normal emittance) was calculated. Figure 4.9 illustrates the wavelength dependent emittance. The highlighted area in Figure 4.9 shows the wavelengths that are associated with temperatures that would be expected to be observed in fires (between 3 – 8 microns corresponds to 362 – 966 Kelvin [81]).

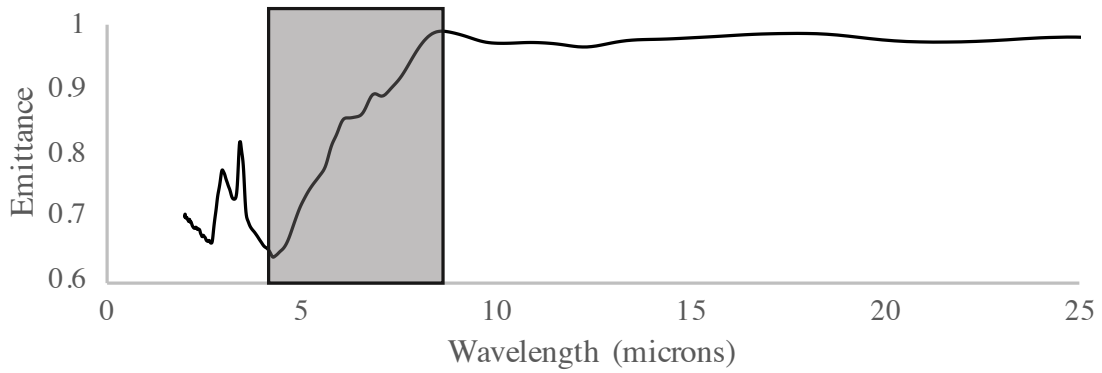


Figure 4.9: Emittance as a function of wavelength.

The emissivity as a function of temperature was calculated up to 1293K using a linear estimation according to Section 2.3.5, and the results are tabulated in Table 4.4.

Table 4.4: Total Near-Normal Emittance

Material	293K	1293K
Safe [®]	0.968	0.782
ComfortBatt [®]	0.957	0.742
Glass wool Insulation	0.974	0.829
Type X Gypsum	0.937	0.787
Type X Gypsum - no paper	0.986	0.853
Wood	0.944	0.843

This method does not take into consideration changes in emissivity as a result of chemical changes, which, there clearly are as illustrated in Figures 4.4, 4.5, 4.6.

4.2.5 Heat Conduction Experiment

This set of experiments used disc-shaped specimens 230mm in diameter and between 54 and 56mm thick cut from slabs of ROCKWOOL Safe[®] insulation, which were placed on a piece of concrete board and exposed to a constant incident heat flux of 25, 35, or 50 kW/m², as described in Section 3.4.4. Throughout each test mass loss of the specimen was measured, and temperature was monitored on the exposed side, the unexposed side, and also on the edge. Figures 4.11, 4.12, and 4.13 illustrate the test data from the cone heater conduction experiments, and Table 4.5 summarizes temperatures after one hour of exposure.






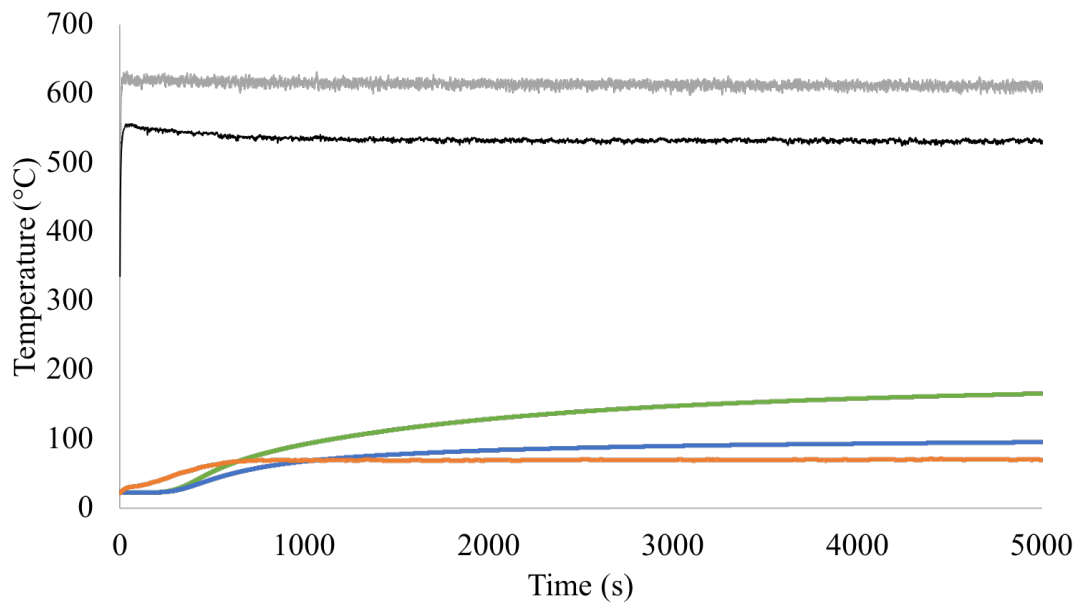
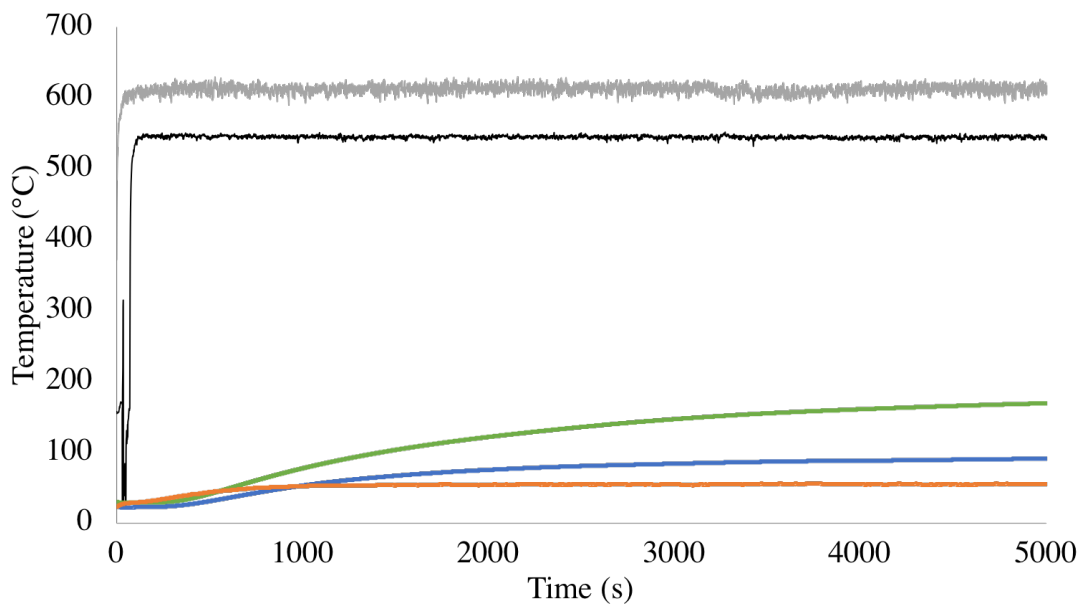
	Exposed side, centerline (TC 1)
	Exposed side, r=7cm (TC 2)
	Unexposed side, centerline (TC 3)
	Unexposed side, r=7cm (TC 4)
	Edge (TC 5)

Figure 4.10: Cone test plots legend.

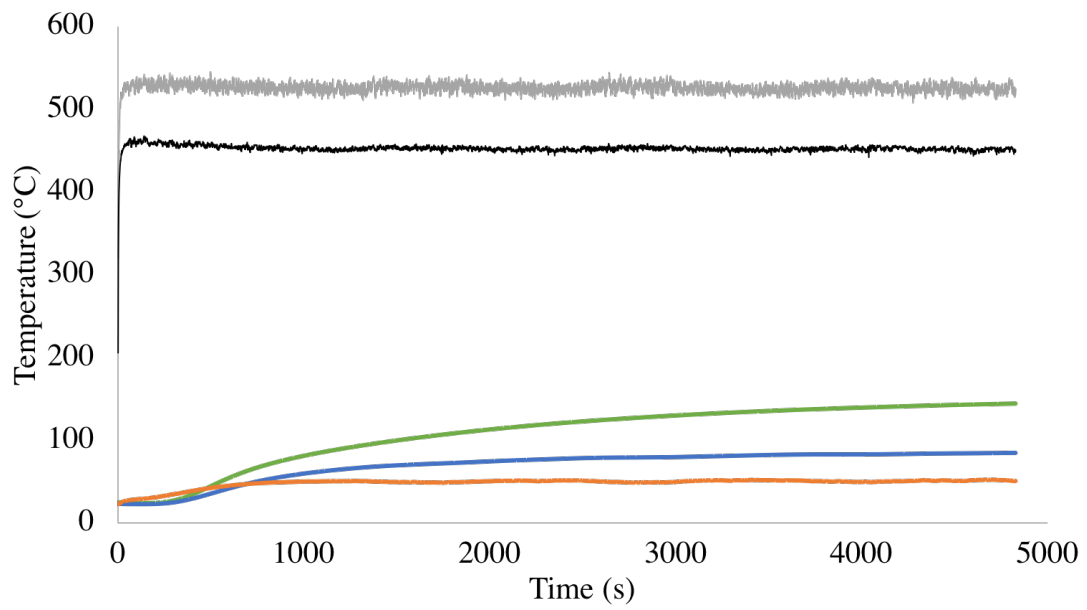


(a) First round

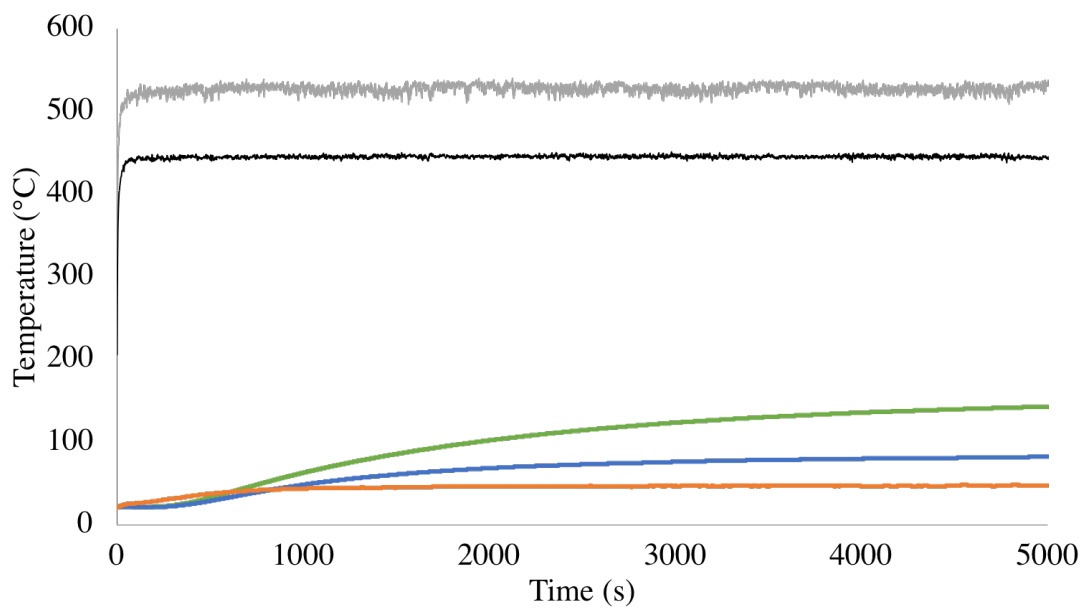


(b) Second round

Figure 4.11: ROCKWOOL Safe[®] under 50kW/m² exposure

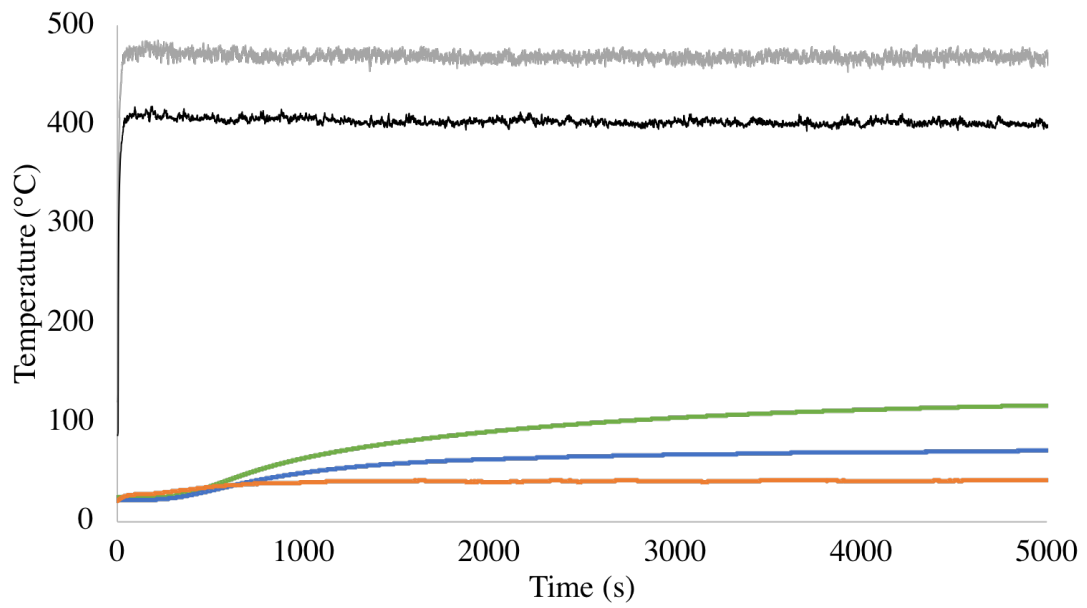


(a) First round

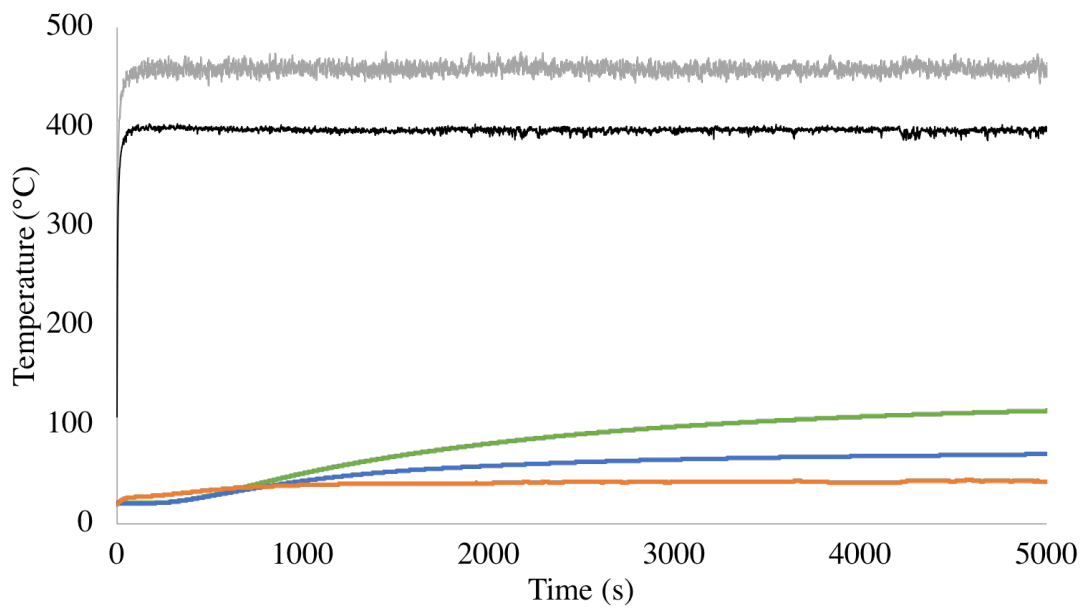


(b) Second round

Figure 4.12: ROCKWOOL Safe[®] under 35kW/m² exposure



(a) First round



(b) Second round

Figure 4.13: ROCKWOOL Safe[®] under 25kW/m² exposure

Table 4.5: Temperatures Measured After 1 Hour During Heat Conduction Experiments (°C)

Incident Heat Flux (kW/m ²)	Round Number	$r = 0$ mm		$r = 70$ mm		T_{EDGE}
		T_{TOP}	T_{BOT}	T_{TOP}	T_{BOT}	
50	1	612	155	531	92	70
50	2	602	156	545	87	55
35	1	527	137	453	83	52
35	2	526	132	443	79	45
25	1	473	110	401	69	42
25	2	458	105	397	68	43

Figure 4.11 illustrates the temperature data when the specimen was exposed to a constant incident heat flux of 50kW/m². Figure 4.11a shows the first round of heating. Surface thermocouples show a sharp increase in temperature immediately on commencement of the test, almost instantaneously reaching 612°C (centreline) and 531°C (7cm from centre), and remaining at that temperature for the duration of the test. The thermocouples on the unexposed side of this specimen show a slower temperature increase with the centreline reaching only 155°C after one hour, and 7cm from the centreline reaching 92°C. The edge of the specimen shows a temperature increase to 70°C by the end of the test. Figure 4.11b shows the data from the second round of heating at 50kW/m². The trends at all temperature measurement points are very similar, with the exposed side temperatures rapidly rising and remaining at a constant temperature throughout the test, and the unexposed side as well as the edge thermocouple rise in temperature much less rapidly. The temperature for the centreline and r=7cm on the exposed side are 602°C and 545°C, almost identical to the first round. The unexposed centreline temperature reaches 156°C and 87°C at r=7cm. The edge temperature reaches 55°C. Most of the temperature points behave the same and reach the same temperatures between the two rounds of tests. The edge and the unexposed side centreline temperatures are notably lower on the second round, which indicates heat was transferring more quickly in all directions in the first round with this exposure.

Figure 4.12 displays the temperature data for the test with constant incident heat flux of 35kW/m². In the first round of heating (Figure 4.12a) the centreline and 7cm

position on the exposed side again increase in temperature immediately to 527°C and 453°C, respectively, and remain approximately at this temperature for the duration of the test. The unexposed side temperatures increase at a slower rate, and reach 137°C (centreline) and 83°C (7cm) by the end of the test. The edge temperature again shows an increase to 52°C, which is an indication of heat loss from the side of the specimen. The temperature measurements from the second round of heating are very similar, and are summarized in Table 4.5, along with results from the 25kW/m² tests.

From the heat conduction experiments, temperatures measured at the locations of interest after 1 hour of exposure are listed in Table 4.5. A 1 hour time frame was chosen since the r=0 position on the unexposed side appeared to be approaching steady state by this time, and other positions had reached steady state. At one hour after the start of exposure, the edge temperatures were significantly less than temperatures on the centreline or at the radial positions of 7cm away from the centre. At the same time, these temperatures were greater than those of ambient air (20–22°C) around the large disk-shaped specimen, suggesting that heat may be transferring from the specimen to ambient by way of convection. Convective heat transfer is proportional to $h \times A \times \Delta T$. In the present study, the heat transfer surface area (in this case, the edge) of the specimen (A) is a maximum of $56\text{mm} \times 2 \times \pi \times 230\text{mm} = 80,927\text{mm}^2 = 0.08927\text{m}^2$ and difference in temperature between the specimen and ambient (ΔT) is a maximum of 50K. Assuming natural convection [78], [79] h would be a maximum of approximately $11\text{Wm}^{-2}\text{K}^{-1}$ (according to calculations outlined in [78]) resulting in convective heat transfer from the side to ambient being approximately $0.08927\text{m}^2 \times 50\text{K} \times 11\text{Wm}^{-2}\text{K}^{-1} = 49\text{W}$.

The distributions shown in Figures 4.11, 4.12, and 4.13 suggest that there were two dimensional conduction effects in the radial direction. Taking a slice through the thickness of the specimen, there were similarly gradients from top to bottom of the slab of insulation. The percent difference between the centreline temperature and that at $r = 7$ cm was 15% on average at the top surface, but 50% on average at the bottom surface.

These results demonstrate that there was a significant thermal gradient in the radial dimension, as well as a significant amount of convective heat loss at the specimen edges. For this type of experiment utilizing a large, symmetric, disc-shaped specimen under a

cone calorimeter (assumed symmetric heat source), a 2-dimensional axi-symmetric model is used to capture the heat transfer through the specimen from the exposed side to the unexposed side, as well as the radial heat transfer.

Figure 4.14 shows the mass loss measured in the cone calorimeter heat conduction experiments as a function of time. For the first round of tests, the average mass loss after 1 hour of exposure was approximately 2%; this value of mass loss is on the same scale as the mass loss measured in TGA tests (Table 4.1), which for the same material had an average value of 1.412%. This is also within range of the tube furnace tests, which resulted in between 1-4% mass loss depending on heating rate. This is an indication that similar decomposition reactions took place despite the different specimen preparation and heating rates. These heated specimens were then allowed to sit in ambient conditions of 20–22°C and 40% relative humidity for a period of 24 hours before the second round of tests, in which the average mass loss after 1 hour of exposure was 1.439%. In the first round of testing, the mass loss rate was still positive after 1 hour of exposure as shown in Figure 4.14, while the mass loss rate was close to zero in the second round, also illustrated in Figure 4.14. These results indicate that the decomposition reactions were largely completed during the first hour that the material was exposed to heat (during round 1 exposure), and few reactions were occurring during heat exposure in round 2. Thus, the values of measured mass loss in round 2 was likely due to residual moisture being driven off the already heat exposed samples of insulation.

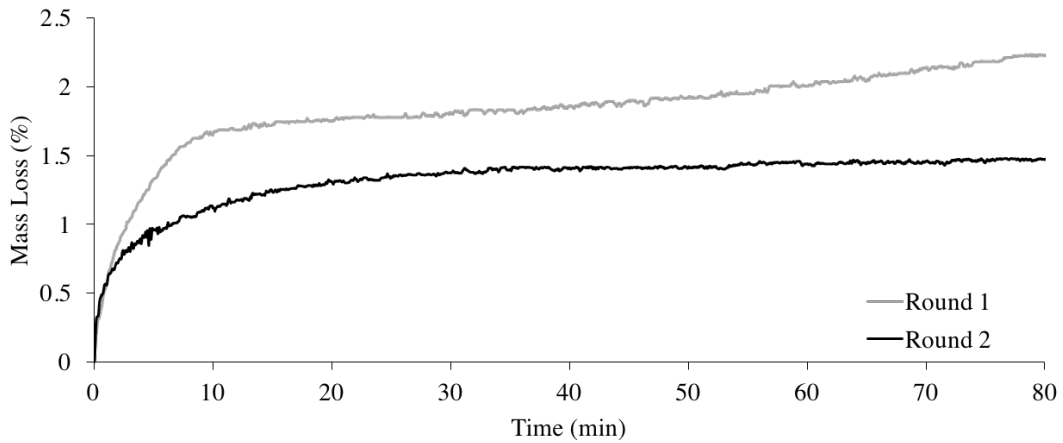


Figure 4.14: Percent Mass Loss During Cone Tests - ROCKWOOL Safe[®]

4.3 Two-Dimensional Axi-Symmetric Model

Key inputs into the numerical model were determined based on measurements conducted during this research, while others were obtained from the literature. These included specific heat, thermal conductivity, emissivity, and density (determined from mass loss).

The average mass loss rate of the insulation over time was determined based on the average of measured percent mass loss determined via the thermal conductivity experiment in Section 3.4.4 and TGA in Section 3.4.1. The mass loss was applied uniformly over time and the volume was assumed to remain constant. The value of thermal conductivity was taken from [23] as a linear approximation. The specific heat and emissivity were also taken as linear approximations using data obtained as described in Sections 3.4.2 and 3.4.3 using ROCKWOOL Safe[®]. Final values are summarized in Table 4.6 below.

Mass loss as a function of exposure time using the cone calorimeter as described in Section 3.4.4 yielded an average mass loss of approximately 2%, and TGA in air as described in Section 3.4.1 resulted in an average mass loss of 1.412%. It was reported by Poljanšek [71] that a similar binder to that used in the MW samples here loses approximately 80% of its mass by the time it is heated to 600°C. The binder content of the mineral wool material

is listed as between 1 and 6% by mass [70]. The predicted mass loss of the binder in the present samples, according to the values reported in [71], should then be between 0.8-4.8%. Assuming that the binder within the mineral wool is the only significant component that contributes to mass loss, the percent mass loss chosen as input for the model should fall within this range. For this model, an average was taken of the two percent mass losses described above from Sections 3.4.4 and 3.4.1 and in the model this percentage was applied uniformly over time.

Thermal conductivity was taken from [23] as a linear approximation. The specific heat and emissivity were also taken as linear approximations using the data obtained as described in Sections 3.4.2 and 3.4.3 using ROCKWOOL Safe®.

Table 4.6: Material properties for the model

Property	Value
Specific Heat	$0.0198T + 4.6915$ J/kgK
Thermal conductivity	$0.0003T + 0.0038$ W/mK
Emissivity	$-0.0002T + 1.0184$
Density	1.710% mass loss, constant volume

All aspects outlined in [78], [79] regarding the characterization of the cone calorimeter were kept the same because this experiment used the same configuration and same equipment. Ambient conditions were adjusted to reflect the conditions in the laboratory at the time of testing.

Following the research in [78], [79], two cone calorimeter experiments were completed using specimens of ROCKWOOL Safe® and results were compared to predictions from the model described in Section 3.5. Figure 4.15 shows a comparison of temperatures with time at the top and bottom of the sample under exposure to 25kW/m² incident flux with the evolution of the bottom surface temperatures with time expanded in the right hand image. Figure 4.16 shows the same comparison for samples exposed to incident flux of 50kW/m².

Steady state values of upper surface temperature show reasonable agreement between model and experiment in the 25kW/m² test, although the experimental and predicted

trends in transient response are different over the first approximately 700 seconds of the test.

The experimental results, as discussed in Section 4.2.5, quickly spike to approximately 450°C at the centreline and slightly cooler, 380°C, at $r=7$ cm within 20 seconds of first exposure to heat. The exposed side appears to reach steady state within approximately 500 seconds to values near 468°C at the centreline and 403°C at $r=7$ cm.

In contrast to the experimental results discussed in more detail in Section 4.2.5, the model predicts that temperatures on the centreline rise quickly to 450°C then continue to increase at a slower rate until reaching a stable value of 488°C after 650 seconds of exposure. In a similar fashion, upper surface temperatures away from the centreline quickly increase to 390°C, then increase to 424°C at a slower rate, again stabilizing at that temperature after approximately 660 seconds. In all cases, values of surface temperature predicted by the model are higher than the comparable experimental value. This temperature difference in predicted and experimental measurements could be due in part to the experimentally determined emissivity inputted into the model. The method used to measure the mineral wool emissivity (Section 3.4.3) does not account for any chemical changes that may occur as a function of temperature. However, it was evident from other characterization experiments (TGA, DSC) that there were notable changes with heating. Measuring emissivity as a function of temperature would impart an additional level of complexity, as there was no method readily available for use at the time of testing. New equipment would have to be purchased or an apparatus would have to be designed, tested, and built in order to carry out such measurements.

Similar to predictions of upper surface temperature, values of lower surface temperature (unexposed side of the sample) are over predicted for both the centerline, $r=0$, and at $r=7$ cm. Trends between experimental data and model predictions are again different in the early stages of heat exposure, as highlighted in the lower plot of Figure 4.15.

While experimental temperatures show very little change between 0 and 300 seconds, the model predicts steadily increasing temperatures with time. After the initial 300 seconds of exposure, however, the shape of the predicted temperature time curve from the model

matches that of the experiments, although the model again over predicts temperatures at every location. The average percent differences between the model predictions and the experimental measurements over the entire data series are outlined in Table 4.7. These suggest that for an exposure of 25kW/m^2 at least, the model captures thermal transfer near the centre of the sample fairly well. Predictions are not nearly as accurate with respect to the radial transfer of heat through the sample from the centre to the edge. The model over predicts the heat transfer from centre to side, which could be due to the centre surface temperature being over predicted initially or the edge boundary condition.

In Figure 4.16, temperatures predicted with the model are compared to experimental measurements made at various locations in the sample for exposures of 50kW/m^2 . The exposed side temperatures are again over predicted, and exhibit differences in trends, over the first 800 seconds, similar to those observed for the 25kW/m^2 exposure results. In this case, however, the temperature predicted at the edge of the sample is in good agreement with measured values, again after the very early transient (first 500 seconds) stage has ended. The experimental results for the unexposed side temperatures exhibit similar discrepancy in trend to those seen for the 25kW/m^2 results, in that the model over predicts the rate at which the unexposed side is initially heated, and also over predicts unexposed side temperatures throughout the simulation, particularly for locations away from the centreline.

Table 4.7: Percent Difference Analysis

Thermocouple	T1	T2	T3	T4	T5
Percent Difference 25 kW/m^2 (%)	3.8	4.9	15	24	34
Percent Difference 50 kW/m^2 (%)	5.4	7.2	8.8	20	3.8

In general, the present model over predicts temperatures in the ROCKWOOL Safe[®] mineral wool insulation samples during heating under a uniform incident surface flux obtained with a cone calorimeter heater. One possible issue could be with the emissivity value used. The method that was used to measure emissivity does not account for chemical changes in the material or any non-linearities in response that might occur at certain temperatures. A higher emissivity in the model could lower the calculated surface tem-

peratures, and consequently lead to prediction of lower bottom temperatures. This could be further investigated by taking emissivity measurements using material that has been previously exposed to high heat, or by finding an apparatus that could take live emissivity measurements as a function of temperature.

The temperature dependent value used in this work for thermal conductivity was taken from the literature for a ROCKWOOL[®] insulation product. It was not specified exactly which product it corresponded to, so this value could have affected modelled results in an unknown way, possibly accounting for some of the over predictions seen in the results.

In the experiment as outlined above, the insulation specimen was placed on top of a concrete board that held two thermocouples. The mineral wool insulation is very light with substantial “air pockets” throughout, and it is possible that there was significant heat transfer interior to the material. In addition, contact between the insulation and the concrete board was not as good as what it would have been in the case of the steel plate, which was used in the initial validation experiment in [78]. This may lead to air gaps between the bottom surface of the mineral wool insulation and the concrete board, resulting in a more complex heat transfer process at that location, which would not be captured in the model.

The main objective of this research was to determine the best methods for characterizing materials for use in full scale fire modelling. In the initial stages of this research simple furnace tests as well as furnace tests following the ASTM E136 method were completed. During these tests, insight into internal degradation, volume change, and temperature changes during heating was gained. These techniques were useful for gaining a general understanding of how the material behaved while being exposed to heat in its virgin form. TGA and DSC are widely used for measuring mass loss and specific heat capacity, respectively, as a function of temperature. For both methods, the material had to be powdered, and only a very small sample was used for testing. This method was relatively quick, easy, and inexpensive. A downside was that this method does not allow for the material to be tested in its virgin form, but it was determined that these were the best methods for measuring their respective properties for mineral wool insulation. In order to determine porosity, Archimedes’ Principle of water displacement was applied. This method worked

reasonably well, however, it also required very small sample sizes in order to fit in the beakers available with sufficient precision for the test. An alternative method such as gas pycnometry could be used in the future to measure porosity of larger samples. The emissivity measurement method used was inexpensive and easy, however, did not account for chemical changes that could occur during heating. Alternative equipment or the incorporation of a furnace to the experimental setup would be beneficial to measure emissivity as a function of temperature while also accounting for chemical changes in the material while being exposed to heat. The heat conduction experiments provided insight on mass loss as well as heat transfer through a larger specimen using an already widely used heat exposure source. This method was useful to cross-check the smaller scale mass loss results and because of the symmetry, relatively straightforward to model.

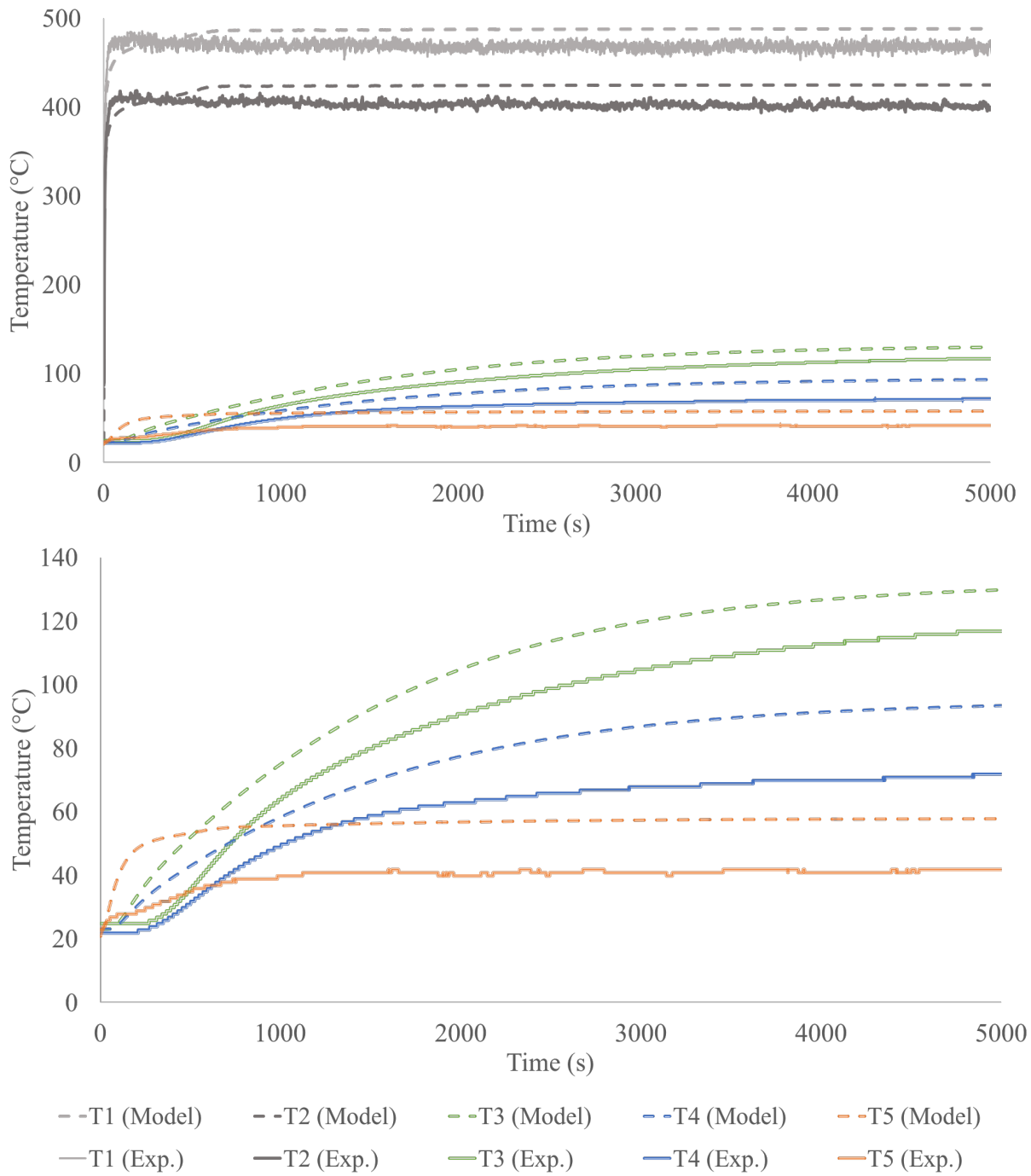


Figure 4.15: Comparison between modelled and experimental results – 25Kw/m².

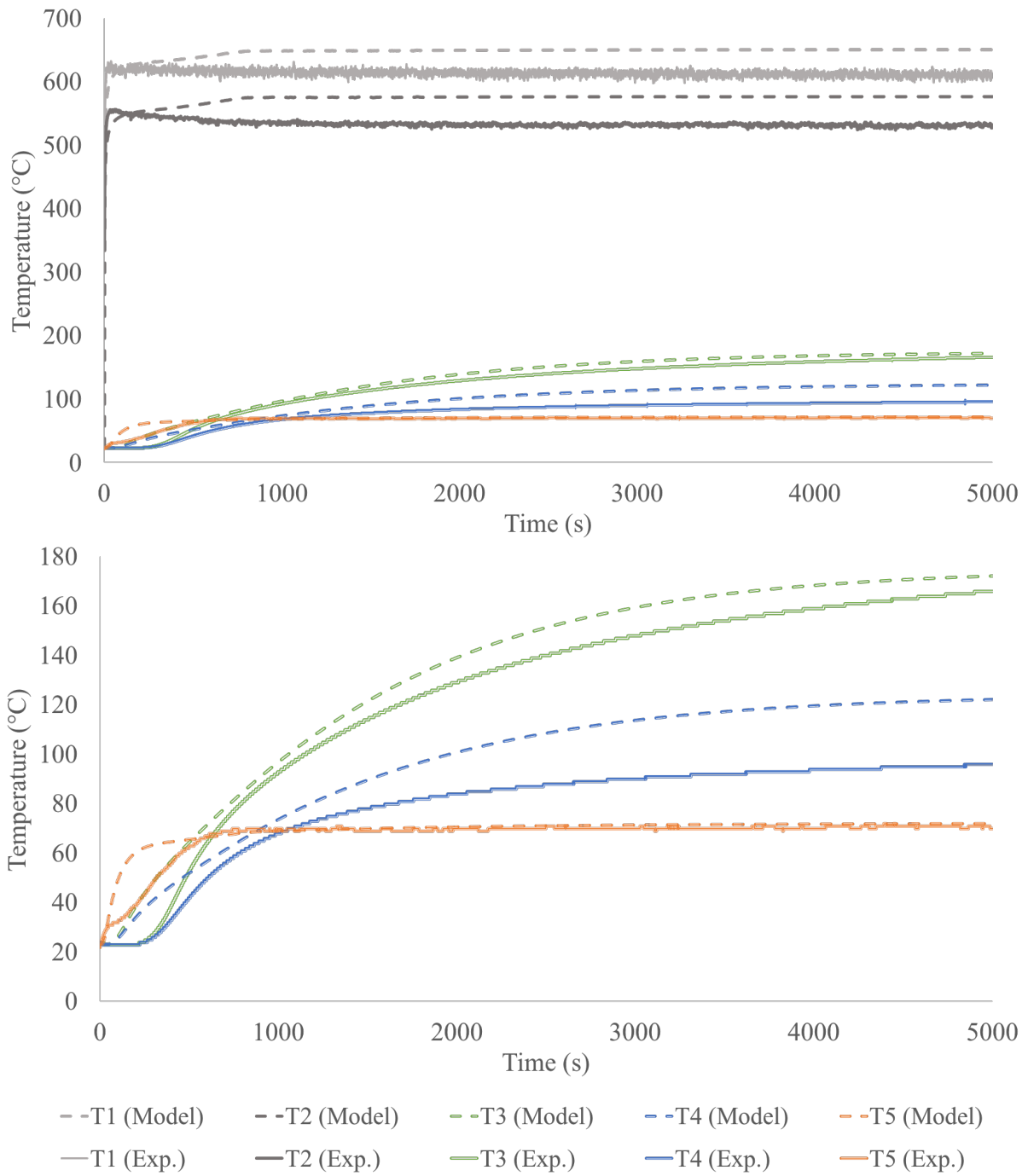


Figure 4.16: Comparison between modelled and experimental results – 50Kw/m².

Chapter 5

Conclusions

During this research, the writer undertook a survey of existing and alternative methods that could be used to characterize mineral wool insulation materials across the range of conditions that would be expected during a fire scenario for the purpose of identifying candidate methods to be used in a future material design assessment tool. Using these methods, the writer conducted an experimental investigation of the thermo-physical and chemical properties of two commonly used insulation materials: ROCKWOOL Safe[®] and ROCKWOOL ComfortBatt[®]. These thermo-physical properties were inputted into a model and compared to results of a larger test system. This section outlines the conclusions of this research.

5.1 Furnace Testing

Two types of furnace tests were conducted on ROCKWOOL Safe[®] fiber insulation in order to gain insight into the temperature dependence and thermochemical degradation of the material. Tests were conducted in a tube furnace at a temperature of 750°C to mimic the conditions of the ASTM E136 combustibility test. From these results, the material was found to meet the temperature rise and mass loss requirements for a non-combustible material. However, at all furnace temperatures above 500°C, closer examination of the

test specimens revealed clear evidence of internal heating in the form of cavities found in the centre of each specimen. Internal heating at lower furnace temperatures causes the material to be classified as combustible, so it would be reasoned that the problem should also be apparent at higher furnace temperatures. However, due to the speed with which the cavity forms and the size of final cavity produced, the centre thermocouple in the specimens exposed in an initially higher temperature furnace was no longer able to follow and record any temperature changes due to the internal self-heating process, and therefore the centre temperature did not appear to exceed the temperature of the furnace. During the tests where the centre temperature was observed to exceed the furnace temperature, the maximum temperatures reached were approximately 500°C, which suggests that the exothermic reactions would only reach that temperature, therefore not having any impact on the furnace tests at higher exposure temperatures. From this, it is concluded that under certain types of heating regimes the mineral wool insulation material could be considered a combustible material while under other conditions would be classified as non-combustible according to ASTM E136. It is possible that the heat released due to combustion reactions is of a similar temperature to the furnace temperature, therefore not resolvable at higher furnace temperatures.

5.2 Characterization Tests

TGA results show mass loss transitions beginning at temperatures between 250–350°C, and there is evidence of reactions with air at temperatures between 400–500°C. DSC results are relatively consistent indicating the onset of temperature induced activity at approximately 200°C in air. In addition, DSC results show a transition at 800°C in air, and in the inert environment there are transitions at approximately 640°C and 840°C. These results imply that there are significant chemical processes occurring during heating, which should be considered when modelling such a material in a fire scenario. The porosity results gave a smaller void fraction for Safe[®] than that of ComfortBatt[®]. The conduction experiment showed a nonlinear thermal gradient through the material with non-negligible heat losses at the edges. In addition, on first heating, the mass loss of the materials surpassed 2.0%

and was continuing to increase even after 1.5 hours of exposure. In heat-exposed material, on the other hand, mass loss appeared to plateau at approximately 1.5%. If this were to be modelled, then a 2D or higher dimensional model accounting for both heat and mass transfer processes is recommended.

Further analysis on DSC curves should be completed to characterize how the binder is breaking down as it is heated, and potentially determine a reaction mechanism. Each peak on a DSC curve represents either an endothermic or exothermic reaction, for which the enthalpy of transition can be calculated. Methods using x-ray diffraction or mass spectrometry could be employed to determine exactly what the material becomes after a transition, or what is emitted as a gas as the material is heated. This reaction mechanism taken together with information regarding mass loss, density, and heat conduction could then be used to create a multiphysics model to predict the behaviour of these insulation materials in fire situations.

5.3 Two-Dimensional Axi-Symmetric Model

Comparison of modelled and experimental results was completed to evaluate the viability of using a coupled experimental-modelling approach to assess thermal transfer through various materials for applications in research and development of construction materials optimized for fire safety. In general, the present model over predicted material temperatures, with the exception of the side temperature during the 50kW/m² test. Further research will be required to determine how to model the contact between the ROCKWOOL Safe® insulation and the concrete board. The model at present does not account for any contact resistance between the materials. There is also potentially an issue with the emissivity value as a function of temperature, since the method used to determine temperature dependent emissivity did not account for chemical changes of the material as it is heated, of which there was evidence of in the other characterization tests such as TGA and DSC. This model, with the aforementioned inputs, is not able to accurately capture the heating phenomena in the transient stage of this experiment.

References

- [1] National Building Code of Canada. Canadian Commission on Building and Fire Codes, Institute for Research in Construction, National Research Council, Ottawa, ON, 2010.
- [2] ASTM Standard E136-12. Standard Test Method for Behavior of Materials in a Vertical Tube Furnace at 750C, ASTM International, West Conshohocken, PA, 2012.
- [3] CAN/ULC-S114. Standard Method of Test for Determination of Non-Combustibility in Building Materials. Underwriters Laboratories of Canada, Ottawa, ON, 2005.
- [4] CAN/ULC-S101. Standard Methods of Fire Endurance Tests of Building Construction and Materials, Underwriters Laboratories of Canada, Toronto, ON, 2014.
- [5] ASTM Standard E119-16a. Standard Test Methods for Fire Tests of Building Construction and Materials, ASTM International, West Conshohocken, PA, 2016.
- [6] Luke Bisby, John Gales, and Cristián Maluk. A contemporary review of large-scale non-standard structural fire testing. *Fire Science Reviews*, 2(1):1, May 2013.
- [7] Steven T Craft, B Isgor, G Hadjisophocleous, and JR Mehaffey. Predicting the thermal response of gypsum board subjected to a constant heat flux. *Fire and Materials: An International Journal*, 32(6):333–355, 2008.
- [8] Georgios K Semitelos, Ioannis D Mandilaras, Dimos A Kontogeorgos, and Maria A Founti. Simplified correlations of gypsum board thermal properties for simulation tools. *Fire and materials*, 40(2):229–245, 2016.

- [9] Dionysios I Kolaitis and Maria A Founti. Development of a solid reaction kinetics gypsum dehydration model appropriate for cfd simulation of gypsum plasterboard wall assemblies exposed to fire. *Fire Safety Journal*, 58:151–159, 2013.
- [10] D Jeulin, P Monnaie, and F Péronnet. Gypsum morphological analysis and modeling. *Cement and Concrete Composites*, 23(2-3):299–311, 2001.
- [11] Yanming Ding, Changjian Wang, and Shouxiang Lu. Modeling the pyrolysis of wet wood using firefoam. *Energy conversion and management*, 98:500–506, 2015.
- [12] Alar Just, Joachim Schmid, and Jürgen König. Post-protection effect of heat-resistant insulations on timber-frame members exposed to fire. *Fire and Materials*, 36(2):153–163, 2012.
- [13] Andrea Frangi, Vanessa Schleifer, and Erich Hugi. A new fire resistant light mineral wool. *Fire technology*, 48(3):733–752, 2012.
- [14] H Takeda. A model to predict fire resistance of non-load bearing wood-stud walls. *Fire and materials*, 27(1):19–39, 2003.
- [15] P Clancy. Advances in modelling heat transfer through wood framed walls in fire. *Fire and materials*, 25(6):241–254, 2001.
- [16] DA Kontogeorgos and MA Founti. A generalized methodology for the definition of reactive porous materials physical properties: Prediction of gypsum board properties. *Construction and Building Materials*, 48:804–813, 2013.
- [17] SUAREZ DIAZ SERGIO. Evaluation of fire safety characteristics of laminated wood panels. Master’s thesis, University of Waterloo, 2015.
- [18] Matthew Didomizio. On the potential use of small scale fire tests for screening steiner tunnel results for spray foam insulation. Master’s thesis, University of Waterloo, 2013.
- [19] Charles T Aire, David A Torvi, and Elizabeth J Weckman. Heat transfer in cone calorimeter tests of generic wall assemblies. In *ASME 2013 International Mechanical*

- Engineering Congress and Exposition*, pages V08AT09A019–V08AT09A019. American Society of Mechanical Engineers, 2013.
- [20] Vytenis Babrauskas. Engineering variables to replace the concept of ‘noncombustibility’. *Fire Technology*, 53(1):353–373, Jan 2017.
- [21] Thomas G Cleary and James G Quintiere. A framework for utilizing fire property tests. *Fire Safety Science*, 3:647–656, 1991.
- [22] ASTM Standard E2226-15b. Standard Practice for Application of Hose Stream, ASTM International, West Conshohocken, PA, 2015.
- [23] Nouredine Benichou, Mohamed A Sultan, Catherine MacCallum, and JK Hum. Thermal properties of wood, gypsum and insulation at elevated temperatures. 2001.
- [24] M.Z. Naser. Properties and material models for modern construction materials at elevated temperatures. *Computational Materials Science*, 160:16 – 29, 2019.
- [25] Nouredine Bénichou and Mohamed A Sultan. Thermal properties of lightweight-framed construction components at elevated temperatures. *Fire and Materials*, 29(3):165–179, 2005.
- [26] JR Mehaffey, P Cuerrier, and G Carisse. A model for predicting heat transfer through gypsum-board/wood-stud walls exposed to fire. *Fire and materials*, 18(5):297–305, 1994.
- [27] H Takeda and JR Mehaffey. Wall2d: A model for predicting heat transfer through wood-stud walls exposed to fire. *Fire and Materials*, 22(4):133–140, 1998.
- [28] H Takeda. A model to predict fire resistance of non-load bearing wood-stud walls. *Fire and materials*, 27(1):19–39, 2003.
- [29] G Thomas. Modelling thermal performance of gypsum plasterboard-lined light timber frame walls using safir and tasef. *Fire and Materials*, 34(8):385–406, 2010.

- [30] Poologanathan Keerthan and Mahen Mahendran. Thermal performance of composite panels under fire conditions using numerical studies: plasterboards, rockwool, glass fibre and cellulose insulations. *Fire Technology*, 49(2):329–356, 2013.
- [31] GQ Li, Jun Han, and Yong C Wang. Constant effective thermal conductivity of intumescent coatings: Analysis of experimental results. *Journal of Fire Sciences*, 35(2):132–155, 2017.
- [32] J Bo Henderson, JA Wiebelt, and MR Tant. A model for the thermal response of polymer composite materials with experimental verification. *Journal of composite materials*, 19(6):579–595, 1985.
- [33] J Su, A Roy-Poirier, P Leroux, PS Lafrance, K Gratton, E Gibbs, and R Berzins. Fire endurance of cross-laminated timber floor and wall assemblies for tall wood buildings. *Conseil national de recherche du Canada, Ottawa, ON*, 2014.
- [34] Thermocouple Sensors. OMEGA Engineering Accessed April 14, 2019, from <https://www.omega.ca/en/resources/thermocouples>, 2018.
- [35] Cheng Qian, Hiroki Ishida, and Kozo Saito. Upward flame spread along pmma vertical corner walls part ii: Mechanism of m shape pyrolysis front formation. *Combustion and Flame*, 99(2):331–338, 1994.
- [36] S Sudheer and SV Prabhu. Characterization of hexane pool fires using infrared thermography. *Journal of fire sciences*, 31(2):143–165, 2013.
- [37] J Meléndez, A Foronda, JM Aranda, F Lopez, and FJ López Del Cerro. Infrared thermography of solid surfaces in a fire. *Measurement Science and Technology*, 21(10):105504, 2010.
- [38] Johan Sjöström and Robert Jansson. Measuring thermal material properties for structural fire engineering. In *from 15th Int Conf on Experimental Mechanics, Porto, 2012*, 2012.

- [39] M Palumbo, J Formosa, and AM Lacasta. Thermal degradation and fire behaviour of thermal insulation materials based on food crop by-products. *Construction and Building Materials*, 79:34–39, 2015.
- [40] Khaled Chetehouna, Naïma Belayachi, Borja Rengel, Dashnor Hoxha, and Philippe Gillard. Investigation on the thermal degradation and kinetic parameters of innovative insulation materials using tga-ms. *Applied Thermal Engineering*, 81:177–184, 2015.
- [41] Seul-Hyun Park, Samuel L Manzello, Dale P Bentz, and Tensei Mizukami. Determining thermal properties of gypsum board at elevated temperatures. *Fire and Materials*, 34(5):237–250, 2010.
- [42] George A Loomis. The porosity and volume changes fire brick at furnace temperatures 1. *Journal of the American Ceramic Society*, 1(6):384–404, 1918.
- [43] Magdaléna Doleželová, Lenka Scheinherrová, Jitka Krejsová, and Alena Vimmrová. Effect of high temperatures on gypsum-based composites. *Construction and Building materials*, 168:82–90, 2018.
- [44] N. Payraudeau Le Roux, S. Meille, J. Chevalier, E. Maire, and J. Adrien. In situ observation of plaster microstructure evolution during thermal loading. *Fire and Materials*, 40(7):973–984.
- [45] Zhenhua Sun and George W. Scherer. Effect of air voids on salt scaling and internal freezing. *Cement and Concrete Research*, 40(2):260 – 270, 2010.
- [46] S Tamari. Optimum design of the constant-volume gas pycnometer for determining the volume of solid particles. *Measurement Science and Technology*, 15(3):549, 2004.
- [47] Seymour Lowell, Joan E Shields, Martin A Thomas, and Matthias Thommes. *Characterization of porous solids and powders: surface area, pore size and density*, volume 16. Springer Science & Business Media, 2012.

- [48] ASTM Standard B923-16. Standard Test Method for Metal Powder Skeletal Density by Helium or Nitrogen Pycnometry, ASTM International, West Conshohocken, PA, 2015.
- [49] ASTM Standard D70-18a. Standard Test Method for Density of Semi-Solid Asphalt Binder (Pycnometer Method), ASTM International, West Conshohocken, PA, 2015.
- [50] ASTM Standard D70-18a. Standard Test Method for Open Cell Content of Rigid Cellular Plastics, ASTM International, West Conshohocken, PA, 2015.
- [51] Laura Espinal. *Porosity and Its Measurement*. John Wiley & Sons, Inc., 2002.
- [52] Franoise Rouquerol, Jean Rouquerol, and Kenneth Sing. Academic Press, London, 1999.
- [53] Shijie Li, Shijie Wang, Xiongyao Li, Yang Li, Shen Liu, and Ian M Coulson. A new method for the measurement of meteorite bulk volume via ideal gas pycnometry. *Journal of Geophysical Research: Planets*, 117(E10), 2012.
- [54] Mette Moesgaard, Hanne D Pedersen, YZ Yue, and ER Nielsen. Crystallization in stone wool fibres. *Journal of Non-Crystalline Solids*, 353(11-12):1101–1108, 2007.
- [55] ASTM Standard E1269-11. Standard Test Method for Determining Specific Heat Capacity by Differential Scanning Calorimetry, ASTM International, West Conshohocken, PA, 2011.
- [56] Nouredine Bénichou and Mohamed A Sultan. Thermal properties of lightweight-framed construction components at elevated temperatures. *Fire and Materials: An International Journal*, 29(3):165–179, 2005.
- [57] ASTM Standard E408-13. Standard Test Methods for Total Normal Emittance of Surfaces Using Inspection-Meter Techniques, West Conshohocken, PA, 2013.
- [58] Nathan A Kotey, John L Wright, and Michael R Collins. A method for determining the effective longwave radiative properties of pleated draperies. *HVAC&R Research*, 17(5):660–669, 2011.

- [59] Donald A Jaworske. Portable infrared reflectometer designed and manufactured for evaluating emittance in the laboratory or in the field. 2000.
- [60] Vanessa Schleifer. *Zum Verhalten von raumabschliessenden mehrschichtigen Holzbauteilen im Brandfall*. PhD thesis, ETH Zurich, 2009.
- [61] Balázs Nagy, Tamás Károly Simon, and Rita Nemes. Effect of built-in mineral wool insulations durability on its thermal and mechanical performance. *Journal of Thermal Analysis and Calorimetry*, pages 1–13.
- [62] C Yang, ME Navarro, B Zhao, G Leng, G Xu, L Wang, Y Jin, and Y Ding. Thermal conductivity enhancement of recycled high density polyethylene as a storage media for latent heat thermal energy storage. *Solar Energy Materials and Solar Cells*, 152:103–110, 2016.
- [63] SV Filimonov, AO Kamaev, ON Shornikova, AP Malakho, and VV Avdeev. Heat-conducting properties of high-temperature materials based on graphite foam. *Refractories and Industrial Ceramics*, 57(2):155–159, 2016.
- [64] Lisha Wang, Michael Gandorfer, Thangaraj Selvam, and Wilhelm Schwieger. Determination of faujasite-type zeolite thermal conductivity from measurements on porous composites by laser flash method. *Materials Letters*, 221:322–325, 2018.
- [65] W. J. Parker, R. J. Jenkins, C. P. Butler, and G. L. Abbott. Flash method of determining thermal diffusivity, heat capacity, and thermal conductivity. *Journal of Applied Physics*, 32(9), 1961.
- [66] S Min, J Blumm, and A Lindemann. A new laser flash system for measurement of the thermophysical properties. *Thermochimica Acta*, 455(1):46–49, 2007.
- [67] Blanket (and Batt) Insulation (COMFORTBATT). Roxul Inc. Accessed March 31, 2015, from http://www.roxul.com/files/RX-NA_EN/pdf/specs/en-ca/072116%20-%20Blanket%20Insulation%20REV%202013-10-28%20ComfortBatt.pdf, 2013.

- [68] Roxul SAFE Technical Data Sheet. Roxul Inc. Accessed May 15, 2017, from http://static.rockwool.com/globalassets/rockwool-na/downloads/technical-data-sheets/commercial/safe_techdatasheet_en.pdf, 2016.
- [69] Roxul ComfortBoard IS Technical Product Information. Roxul Inc. Accessed March 31, 2015, from http://www.roxul.com/files/RX-NA_EN/pdf/Technical%20Data%20Sheets-%20updated/Building%20Envelope/ComfortBoard%20IS.pdf, 2014.
- [70] Roxul Material Safety Data Sheet. Roxul Inc. Accessed March 16, 2016, from http://www.roxul.com/files/RX-NA_EN/pdf/MSDS%20and%20Safety%20Bulletin/Roxul%20Material%20Safety%20Data%20Sheet%2002-13-14.pdf, 2014.
- [71] Ida Poljanšek, Urška Šebenik, and Matjaž Krajnc. Characterization of phenol–urea–formaldehyde resin by inline ftir spectroscopy. *Journal of applied polymer science*, 99(5):2016–2028, 2006.
- [72] Type K Thermocouple. REOTEMP Instruments Corporation Accessed June 27, 2017, from <http://www.thermocoupleinfo.com/type-k-thermocouple.htm>, 2011.
- [73] Users manual FLIR T6xx series. FLIR Systems, Inc. Accessed July 29 2019, from <https://www.flir.ca/globalassets/imported-assets/document/flir-t6xx-series-user-manual.pdf>.
- [74] VV Calmidi and RL Mahajan. The effective thermal conductivity of high porosity fibrous metal foams. *Journal of Heat Transfer*, 121(2), 1999.
- [75] TGA Thermogravimetric Analyzer Q Series Getting Started Guide. TA Instruments – Waters LLC Accessed November 12 2019, from <https://www.usf.edu/research-innovation/rf/usf-connect/documents/tga-q500.pdf>.
- [76] ASTM Standard E967-08. Standard Test Method for Temperature Calibration of Differential Scanning Calorimeters and Differential Thermal Analyzers, ASTM International, West Conshohocken, PA, 2008.

- [77] ASTM Standard E968-02. Standard Practice for Heat Flow Calibration of Differential Scanning Calorimeters, ASTM International, West Conshohocken, PA, 2002.
- [78] Daniel Pegg Wilson. Numerical simulations of small-scale and full-scale fire experiments. Master's thesis, University of Waterloo, 2018.
- [79] M. DiDomizio, D. Wilson, E. Weckman, and C. Devaud. A modified cone calorimeter experiment for study of pyrolysis.
- [80] KS Hwang and TH Tsou. Thermal debinding of powder injection molded parts: Observations and mechanisms. *Metallurgical transactions A*, 23(10):2775–2782, 1992.
- [81] Neil Sellers. *Handbook of Terahertz Technology*. Scientific e-Resources, 2018.
- [82] Stevenson. Oxford dictionary of english. Oxford University Press. Accessed March 31, 2015, from <http://www.oxfordreference.com/10.1093/acref/9780199571123.001.0001/acref-9780199571123>.
- [83] Blanket (and Batt) Insulation (COMFORTBATT) Technical Data Sheet. Roxul Inc. Accessed May 15, 2017, from <http://static.rockwool.com/globalassets/rockwool-na/downloads/technical-data-sheets/residential/technical-data-sheet-comfortbatt-canada.pdf>, 2016.
- [84] Roxul Product Information. Roxul Inc. Accessed May 15, 2017, from <http://www.roxul.com/>, 2016.
- [85] Michel Goossens, Frank Mittelbach, and Alexander Samarin. *The L^AT_EX Companion*. Addison-Wesley, Reading, Massachusetts, 1994.
- [86] Donald Knuth. *The T_EXbook*. Addison-Wesley, Reading, Massachusetts, 1986.
- [87] Leslie Lamport. *L^AT_EX — A Document Preparation System*. Addison-Wesley, Reading, Massachusetts, second edition, 1994.

- [88] N Ryder and E Weckman. Effects of convective heat transfer coefficient in prediction of materials properties from cone calorimeter testing. *Fire and Materials*, pages 379–388, 2013.
- [89] P. Hartlieb, M. Toifl, F. Kuchar, R. Meisels, and T. Antretter. Thermo-physical properties of selected hard rocks and their relation to microwave-assisted comminution. *Minerals Engineering*, 91(Supplement C):34 – 41, 2016. Physical Separation.
- [90] Karl Stephan and A Laesecke. The thermal conductivity of fluid air. *Journal of physical and chemical reference data*, 14(1):227–234, 1985.
- [91] Georgios K Semitelos, Ioannis D Mandilaras, Dimos A Kontogeorgos, and Maria A Founti. Simplified correlations of gypsum board thermal properties for simulation tools. *Fire and materials*, 40(2):229–245, 2016.
- [92] DA Kontogeorgos and MA Founti. A generalized methodology for the definition of reactive porous materials physical properties: Prediction of gypsum board properties. *Construction and Building Materials*, 48:804–813, 2013.